



11-27-2019

Characterization of the role of BGS13 in the secretory mechanism of *Pichia pastoris*

Christopher A. Naranjo
University of the Pacific, c_naranjo@u.pacific.edu

Anita Jivan
University of the Pacific, a_jivan@u.pacific.edu

Maria N. Vo
University of the Pacific

Katherine de Sa Campos
University of the Pacific

Jared S. Devarmin
University of the Pacific

See next page for additional authors

Follow this and additional works at: <https://scholarlycommons.pacific.edu/cop-facarticles>

 Part of the [Life Sciences Commons](#)

Recommended Citation

Naranjo, C. A., Jivan, A., Vo, M. N., de Sa Campos, K., Devarmin, J. S., Hekman, R., Uribe, C., Hang, A., Her, K., Fong, M. M., Choi, J. J., Chou, C., Rabara, T., Myers, G., Moua, P. S., Thor, D., Risser, D. D., Vierra, C., Franz, A., Lin-Cereghino, J., & Lin-Cereghino, G. (2019). Characterization of the role of BGS13 in the secretory mechanism of *Pichia pastoris*. *Applied and Environmental Microbiology*, 85(24), e01615–e01619. DOI: [10.1128/AEM.01615-19](https://doi.org/10.1128/AEM.01615-19)
<https://scholarlycommons.pacific.edu/cop-facarticles/864>


This Article is brought to you for free and open access by the All Faculty Scholarship at Scholarly Commons. It has been accepted for inclusion in College of the Pacific Faculty Articles by an authorized administrator of Scholarly Commons. For more information, please contact mgibney@pacific.edu.

Authors

Christopher A. Naranjo, Anita Jivan, Maria N. Vo, Katherine de Sa Campos, Jared S. Devarmin, Ryan Hekman, Christina Uribe, Aaron Hang, Kai Her, Michelle M. Fong, Joyce J. Choi, Caroline Chou, Taylor Rabara, Gina Myers, Pachai S. Moua, Der Thor, Douglas D. Risser, Craig Vierra, Andreas Franz, Joan Lin-Cereghino, and Geoff Lin-Cereghino



Role of *BGS13* in the Secretory Mechanism of *Pichia pastoris*

Christopher A. Naranjo,^a Anita D. Jivan,^a Maria N. Vo,^a Katherine H. de Sa Campos,^a Jared S. Deyarmin,^a Ryan M. Hekman,^a Christina Uribe,^a Aaron Hang,^a Kai Her,^a Michelle M. Fong,^a Joyce J. Choi,^a Caroline Chou,^a Taylor R. Rabara,^b Gina Myers,^a Pachai Moua,^a Der Thor,^c  Douglas D. Risser,^a Craig A. Vierra,^a Andreas H. Franz,^b Joan Lin-Cereghino,^a Geoff P. Lin-Cereghino^a

^aDepartment of Biological Sciences, University of the Pacific, Stockton, California, USA

^bDepartment of Chemistry, University of the Pacific, Stockton, California, USA

^cDepartment of Biomedical Sciences, Arthur A. Dugoni School of Dentistry, University of the Pacific, San Francisco, California, USA

ABSTRACT The methylotrophic yeast *Pichia pastoris* has been utilized for heterologous protein expression for over 30 years. Because *P. pastoris* secretes few of its own proteins, the exported recombinant protein is the major polypeptide in the extracellular medium, making purification relatively easy. Unfortunately, some recombinant proteins intended for secretion are retained within the cell. A mutant strain isolated in our laboratory, containing a disruption of the *BGS13* gene, displayed elevated levels of secretion for a variety of reporter proteins. The Bgs13 peptide (Bgs13p) is similar to the *Saccharomyces cerevisiae* protein kinase C 1 protein (Pkc1p), but its specific mode of action is currently unclear. To illuminate differences in the secretion mechanism between the wild-type (wt) strain and the *bgs13* strain, we determined that the disrupted *bgs13* gene expressed a truncated protein that had reduced protein kinase C activity and a different location in the cell, compared to the wt protein. Because the Pkc1p of baker's yeast plays a significant role in cell wall integrity, we investigated the sensitivity of the mutant strain's cell wall to growth antagonists and extraction by dithiothreitol, determining that the *bgs13* strain cell wall suffered from inherent structural problems although its porosity was normal. A proteomic investigation of the *bgs13* strain secretome and cell wall-extracted peptides demonstrated that, compared to its wt parent, the *bgs13* strain also displayed increased release of an array of normally secreted, endogenous proteins, as well as endoplasmic reticulum-resident chaperone proteins, suggesting that Bgs13p helps regulate the unfolded protein response and protein sorting on a global scale.

IMPORTANCE The yeast *Pichia pastoris* is used as a host system for the expression of recombinant proteins. Many of these products, including antibodies, vaccine antigens, and therapeutic proteins such as insulin, are currently on the market or in late stages of development. However, one major weakness is that sometimes these proteins are not secreted from the yeast cell efficiently, which impedes and raises the cost of purification of these vital proteins. Our laboratory has isolated a mutant strain of *Pichia pastoris* that shows enhanced secretion of many proteins. The mutant produces a modified version of Bgs13p. Our goal is to understand how the change in the Bgs13p function leads to improved secretion. Once the Bgs13p mechanism is illuminated, we should be able to apply this understanding to engineer new *P. pastoris* strains that efficiently produce and secrete life-saving recombinant proteins, providing medical and economic benefits.

KEYWORDS *Pichia pastoris*, cell wall, mass spectrometry, recombinant DNA technology, recombinant protein production, secretion

The methylotrophic yeast *Pichia pastoris* (also called *Komagataella pastoris*) is a popular host for recombinant protein expression. The yeast has been genetically engineered to express over 5,000 heterologous proteins and has been valued for industrial, pharmaceutical, and basic research purposes for the past 25 years (1, 2). In

Citation Naranjo CA, Jivan AD, Vo MN, de Sa Campos KH, Deyarmin JS, Hekman RM, Uribe C, Hang A, Her K, Fong MM, Choi JJ, Chou C, Rabara TR, Myers G, Moua P, Thor D, Risser DD, Vierra CA, Franz AH, Lin-Cereghino J, Lin-Cereghino GP. 2019. Role of *BGS13* in the secretory mechanism of *Pichia pastoris*. *Appl Environ Microbiol* 85:e01615-19. <https://doi.org/10.1128/AEM.01615-19>.

Editor Irina S. Druzhinina, Nanjing Agricultural University

Copyright © 2019 American Society for Microbiology. All Rights Reserved.

Address correspondence to Geoff P. Lin-Cereghino, glincere@pacific.edu.

Received 20 July 2019

Accepted 22 September 2019

Accepted manuscript posted online 4 October 2019

Published 27 November 2019

fact, more than 70 *P. pastoris* products, ranging from anticancer therapeutics to vaccine antigens, are commercially available or in late-stage development (phase 2 or phase 3 clinical trials) (3, 4). Because *P. pastoris* secretes few of its own proteins, the expressed recombinant protein is usually the major polypeptide species found in the extracellular medium (ECM). Thus, programmed export acts as a valuable step in the purification of the heterologous protein and is considered a strong asset of this microbial host. Unfortunately, one of the greatest weaknesses of the system is that some recombinant proteins that are engineered to be secreted are retained or degraded inside the cell (5, 6). Furthermore, these heterologous proteins may lack the correct posttranslational modifications and folding of the native proteins, which may cause problems, including reduced activity and triggering of an immune response if injected into the human body.

To illuminate the mechanism of *P. pastoris* secretion and to help alleviate the problem of inefficient protein export, we identified 13 β -galactosidase supersecretion (BGS) genes through a selection of genomic disruption mutants generated by using a restriction enzyme-mediated integration (REMI) plasmid (7). In these selected mutants, the pREMI plasmid was inserted into a chromosomal gene whose modified function led to an increase in β -galactosidase secretion. The enhanced secretion of this enzyme enabled the mutated cells to metabolize lactose, allowing the mutants to be selected on lactose-containing medium. The affected genes appear to have functions in intracellular signaling or vesicle transport. One particular mutant strain, the *bgs13* strain, showed enhanced secretion of the majority of recombinant proteins tested. Because most supersecreting mutant strains identified by other laboratories demonstrated enhanced secretion of only a small subset of peptides (8), the *bgs13* mutant raised the intriguing possibility of being a universal supersecretor.

The Bgs13 polypeptide (Bgs13p) shares similarities with protein kinase C (PKC) 1 protein (Pkc1p) from the yeast *Saccharomyces cerevisiae*. The predicted amino acid sequence of wild-type (wt) *P. pastoris* Bgs13p is 50% identical and 68% similar to that of *S. cerevisiae* Pkc1p in the N-terminal region. In baker's yeast, Pkc1p plays a critical role in the cell wall integrity (CWI) pathway, which is responsible for detecting and responding to cell wall stress that arises under normal growth conditions or through environmental challenges (9, 10). The CWI pathway in *S. cerevisiae* relies on a family of cell surface sensors coupled to a small G protein, Rho1p, which is considered to be the master regulator of CWI signaling not only because it senses signals from the cell surface but also because it influences a variety of mechanisms involved in cell wall biogenesis, actin organization, and polarized secretion (10). The transcriptional output of the CWI pathway is under the control of a mitogen-activated protein kinase (MAPK) cascade dependent on Pkc1p, which interacts with Rho1p. Pkc1p induces the activity of the MAPK cascade by phosphorylating Bck1, which stimulates a redundant pair of kinases, Mkk1 and Mkk2, that finally regulate Slr2/Mpk1. Ultimately, Slr2/Mpk1 interacts with Rlm1p to regulate transcriptional responses of cell wall genes on an intricate, global scale; some responses are positive, while others are negative (11). Like the Δ *pkc1* strain of baker's yeast, the *bgs13* strain of *P. pastoris* released more alkaline phosphatase (a vacuolar enzyme) than its wt parent, suggesting a more permeable cell wall than normal (7). For both species, alkaline phosphatase export was inhibited by the addition of sorbitol to the medium, strongly suggesting that CWI was compromised by the variant *bgs13p* function. Interestingly, in *S. cerevisiae*, the loss of *PKC1* resulted in a more severe growth defect than that produced by deletion of any of the members of the MAPK cascade under the control of this kinase, which suggests that Pkc1p regulates additional steps along the CWI pathway (10).

Although several lines of evidence point to modification of the cell wall as the cause of enhanced secretion in the *bgs13* strain, some previous results suggest that other factors may be involved (7). For example, unlike the *S. cerevisiae* Δ *pkc1* strain, *bgs13* strain cells did not require the presence of 1 M sorbitol in the medium for growth. This result raised the question of whether pREMI insertion into the *BGS13* locus caused only a partial loss of function. In addition, other experimental results implicated Bgs13p in

the protein-sorting process. For instance, studies using the α -mating factor secretion signal sequence fused to an N-terminal maltose-binding protein (MBP) and a C-terminal enhanced green fluorescent protein (EGFP) indicated that the hybrid protein was proteolyzed at the linker region between the two domains prior to secretion. Compared to the wt strain, the *bgs13* mutant increased the secretion of MBP-EGFP while decreasing its proteolysis in the linker region between the two domains (12). Furthermore, fluorescence microscopy indicated that, in the wt background, MBP-EGFP gave rise to green fluorescence mainly in the vacuole, while the *bgs13* allele caused MBP-EGFP to be shunted from the vacuole and localized to other parts of the secretory network prior to its export into the ECM. The suppression of vacuolar targeting has been linked to increased secretion in baker's yeast and *P. pastoris* (13, 14). Thus, it is not clear whether changes in cell wall structure are (i) the cause of increased secretion of proteins or (ii) an effect of *bgs13* mutant protein activity that is not directly responsible for enhanced peptide export.

To help resolve this question, we have focused on characterizing the genetic nature of the chromosomal *bgs13* mutation, determining whether it yields complete or partial loss of function, and illuminating how this mutation affects the localization and kinase activity of its gene product. In addition, we have examined how the mutation affects the population of secreted proteins, as well as the constituents of the cell wall. Taken together, these results provide clues for comprehending how the mutation in the *bgs13* strain triggers enhanced protein secretion.

RESULTS AND DISCUSSION

Characterization of mutant *bgs13* mRNA. The *bgs13* mutant strain was generated by the insertion of the 2.8-kb pREMI plasmid into the locus (7). The *bgs13* strain had no obvious phenotypic difference in growth, compared to its wt parent, except that its doubling time was about 50% longer. We initially hypothesized that the mutant *P. pastoris bgs13* strain was not a null strain, since, unlike the $\Delta pkc1$ strain of baker's yeast (15), it could grow without osmotic stabilization and appeared to have normal architecture inside its cells, based on transmission electron microscopy analysis (7). Therefore, it was postulated that the insertion of pREMI into the *BGS13* locus did not cause a gene knockout but allowed for the expression of a Bgs13p variant. To determine whether *BGS13* mRNA was present inside the *bgs13* strain cells, we first examined the genomic DNA from the *bgs13* strain obtained by a plasmid rescue strategy (7, 16). Genomic DNA 5' and 3' of the pREMI plasmid insertion indicated that the vector had integrated within the codon 147 of the *BGS13* open reading frame (ORF) (between nucleotide 441 and nucleotide 442) (Fig. 1A and B). We reasoned that either or both of two hybrid mRNAs could be produced, one driven by the *BGS13* promoter, containing only the 5' end of the *BGS13* mRNA, with the first 147 codons, and the 3' sequence from the pREMI plasmid (Fig. 1B, left), and/or one driven by a promoter within the pREMI plasmid, containing 5' plasmid sequence fused to codons 148 through 1035 of the *BGS13* gene at the 3' end (Fig. 1B, right). We hypothesized that either mRNA could potentially encode a protein with some form of residual Bgs13p activity that would promote supersecretion.

To distinguish between these two possibilities, total mRNA from wt and *bgs13* strain cells (grown under either glucose or methanol conditions) was reverse transcribed, and the resulting cDNA was subjected to PCR amplification with primer combinations annealing to either the 5' region or the 3' region of the *BGS13* ORF (Fig. 1A and B). A PCR product of the expected size (approximately 650 bp) was synthesized with primers annealing to the 3' end of the *BGS13* coding sequence using cDNA produced from the wt strain and the *bgs13* strain, indicating that mRNA containing the 3' region of *BGS13* was found at significant levels inside the *bgs13* strain cells (Fig. 1B, right, and Fig. 1C). A PCR product of approximately 500 bp was synthesized with primers annealing to the 5' end of the *BGS13* coding sequence from cDNA produced by the wt strain but not the *bgs13* strain, indicating that the *bgs13* strain cells did not contain mRNA containing the 5' region of *BGS13* (Fig. 1B, right, and Fig. 1D).

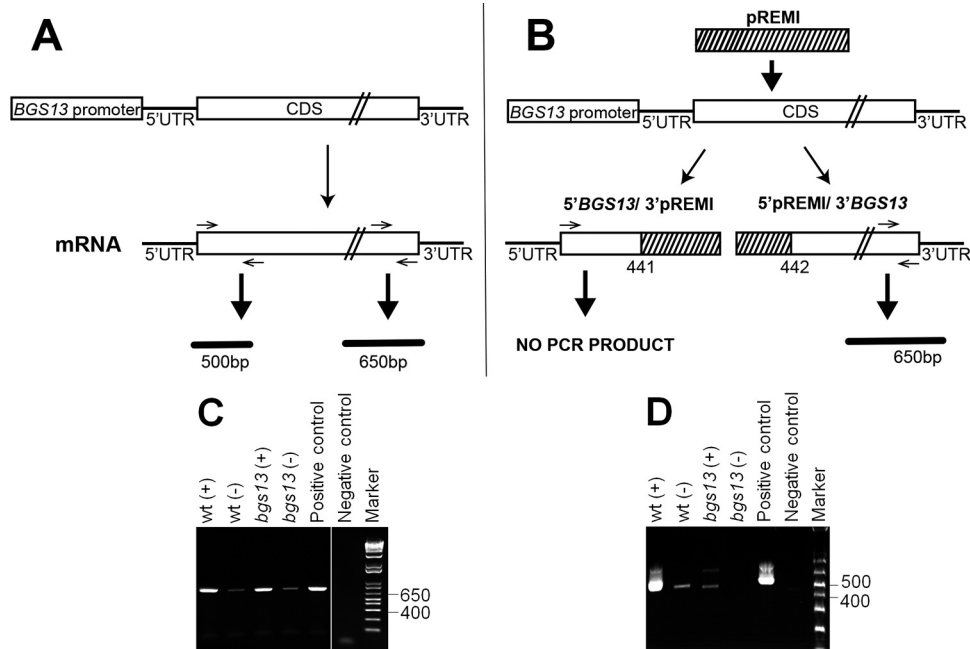


FIG 1 PCR analysis used to determine the structure of the wt and *bgs13* mRNA in mutant cells. (A and B) Schematics show the PCR used to determine the regions of the *BGS13* sequence present in the wt (A) and *bgs13* (B) strain mRNAs. Primers annealing to the 5' end of the *BGS13* cDNA should amplify a 500-bp product, while primers annealing to the 3' end of the *BGS13* cDNA should amplify a 650-bp product. CDS, coding sequence. (C and D) cDNA reactions were performed on total RNA isolated from wt and *bgs13* strain cells. +, reaction mixture containing reverse transcriptase; -, reaction mixture lacking reverse transcriptase. Primers annealed to either the 3' end (C) or the 5' end (D) of the *BGS13* gene. Plasmids containing the entire *BGS13* gene or no recombinant gene served as the templates for the positive- and negative-control reactions, respectively. For clarity, duplicate samples and some extraneous controls were spliced out of the image shown in panel C.

mRNA containing the 5' *BGS13* sequence might have been transcribed in the *bgs13* strain cells but most likely was degraded due to an early termination codon created in the fusion of the *BGS13* and pREMI sequences, which triggered the up frameshift (UPF) mechanism (17). As negative controls, cDNA reactions that lacked reverse transcriptase did not yield significant amounts of either 5' or 3' PCR products, as expected (Fig. 1C and D); the weak bands were most likely amplified from undigested genomic DNA. Thus, the *bgs13* strain cells contained a stable mRNA transcribed from the 3' region of the *BGS13* gene.

Cloning of *Remi-bgs13* cDNA. Our next step was to determine the sequence of the hybrid mRNA, which was hypothesized to contain the 5' pREMI sequence fused to the *BGS13* sequence 3' of codon 147. Using a modified 5'-rapid amplification of cDNA ends (5'-RACE) strategy with a commercially available kit, we first reverse transcribed total RNA using a 5' random primer mix. The reverse transcriptase added several nontemplated residues to the 3' end of the cDNA products. An oligonucleotide annealing to these nontemplated residues was used by the reverse transcriptase to synthesize the complementary second cDNA strand. A 5'-RACE reaction was then performed with a primer that annealed near nucleotide 1200 of the *BGS13* coding sequence and a kit-provided universal primer mix (UPM) that annealed to the nontemplated bases. A smeared 800- to 1,500-bp PCR product, which was seen only in reactions with both primers and not in those with the individual primers, was produced in this first 5'-RACE reaction (Fig. 2, lane 1).

A second nested PCR was then performed on this reaction product, using a primer that annealed near nucleotide 1000 of the *BGS13* coding sequence and the UPM. The two PCR products (approximately 800 bp and 1,100 bp) resulting from this amplification reaction (Fig. 2, lanes 2 and 3) were then gel purified and cloned into a sequencing vector. While the 1,100-bp product contained no *BGS13* or pREMI sequence, the 800-bp

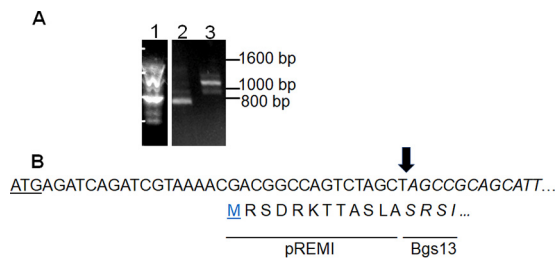


FIG 2 Cloning of *bgs13* strain cDNA. (A) Lane 1, product of 5' RACE reaction; lane 2, 800-bp product of nested PCR after gel isolation; lane 3, 1,100-bp product of nested PCR after gel isolation. (B) Sequence of the Remi-*bgs13* cDNA, which contains 12 codons from pREMI (nonitalicized) fused in frame to codon 148 and the remainder of the *BGS13* coding sequence (italicized). The start codon is underlined. The arrow indicates the border between pREMI and *BGS13* DNA sequence. The predicted protein sequence is shown below the DNA sequence. In the protein sequence, the amino acids encoded by pREMI are nonitalicized, while the residues resulting from *BGS13* coding sequence are italicized.

sequence, which represented the *Remi-bgs13* hybrid transcript, contained a 5' untranslated region (UTR) and 12 codons (initiated by an ATG) originating from the pREMI plasmid, fused in frame to codon 148 to the stop codon of the *BGS13* coding sequence (Fig. 2). The resultant protein, designated Remi-*bgs13p*, was presumed to have some Bgs13p activity and to be responsible for the supersecretor phenotype. Similarly to *Saccharomyces cerevisiae* Pkc1p, *P. pastoris* Remi-*bgs13p*, due to the lack of its first 147 amino acids, does not contain a homologous region 1 (HR1) domain (15). In baker's yeast, the HR1 domain of Pkc1p is associated with (i) binding to Rho1p, the upstream activator of Pkc1p, and (ii) the regulation of oligosaccharyltransferase activity and actin depolarization. However, Remi-*bgs13p* contains domains such as the C1 domain, which is involved in the control of the transcription of cell wall genes and Rho1p binding, as well as its kinase domain (18).

Creation of a null *bgs13* strain. To reveal the effect of inhibiting all Bgs13p activity on secretion, we then endeavored to create a null *bgs13* strain. Attempts to knock out the *BGS13* gene, using two different strategies, were unsuccessful. First, using the traditional technique, a knockout construct was created with approximately 500 nucleotides of *BGS13* regions upstream and downstream of its coding sequence (19, 20). These regions flanked a central selectable marker, *Saccharomyces cerevisiae* *HIS4*. His⁺ transformants of the yDT39 (*met2 his4*) strain were generated, but PCR analysis of genomic DNA indicated that none of them contained the expected disruption/deletion of the chromosomal *BGS13* (data not shown). Recombination at sites lacking homology is dependent on the targeted gene in *P. pastoris* (21). As a second strategy, a CRISPR technique optimized for *P. pastoris* (22) was used. Six CRISPR vectors, with a Zeocin- or G418-selectable marker, contained guide RNA (gRNA) sequences that targeted three different stretches of the coding region (positions +816 to +836, +1049 to +1068, and +1069 to +1088) responsible for the N terminus of Bgs13p. Zeocin- and G418-resistant transformants were selected on medium supplemented with 1 M sorbitol in case the Bgs13 knockout resulted in cell wall dysfunction, which is true of the baker's yeast Δ *pkc1* strain (15). Genomic DNA from the targeted *BGS13* region in 60 randomly selected transformants was amplified by PCR and sequenced. Approximately one-third of the colonies contained genomic mutations within the *BGS13* sequence, but all were either 3- or 6-bp deletions in the *BGS13* coding region (data not shown). Because none of these deletions resulted in frameshifts, the DNA could encode Bgs13p lacking 1 or 2 amino acids at most, most likely retaining some Bgs13p activity. This inability to create a null mutant strongly suggests that the *BGS13* gene is essential for viability. Therefore, we had to proceed in our studies without the use of a *BGS13* knockout strain.

Examining the PKC activity of wt Bgs13p and mutant Bgs13p. Our next step was to compare the effects of wt Bgs13p and Remi-*bgs13p*, to characterize the relationship between their functional activities and their effects on secretion efficiency. Due to its homology to *S. cerevisiae* *PKC1*, we hypothesized that the *BGS13* gene product would

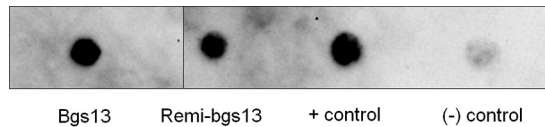


FIG 3 Production of Bgs13p and Remi-bgs13p. Strains expressing the wt Bgs13p, Remi-bgs13p, or no recombinant protein were grown on glucose, induced with methanol, and harvested. Both proteins were expressed with a *c-myc* epitope. Intracellular extracts were isolated, and equal amounts of protein were used in a spot Western blot analysis. Protein extracts and controls were probed with an anti-*c-myc* antibody. Spot Western blot images captured with a Chemilmager 5500 were quantified with integrated density value (IDV) analysis. $-$, wt strain carrying an empty pPICZB plasmid; $+$, 20 ng of a commercially available, *c-myc*-tagged, control protein. For clarity, duplicate samples were spliced out of the image.

have PKC activity. While a deletion in its N terminus would remove the HR1 domain, the mutant peptide should contain its putative kinase domain. We sought to compare the protein kinase activities of the Bgs13p and Remi-bgs13p.

A commercially available kit detected only very low PKC activity in intracellular extracts from the wt strain, which could not be distinguished from the levels in *bgs13* strain cells, helping to establish a baseline of activity. Both wt Bgs13-*c-myc*-His₆ (pKdSC5) and Remi-bgs13-*c-myc*-His₆ (pAH1) were expressed from an *AOX1* promoter in wt cells that first were grown on repressing glucose medium and then were induced on methanol growth medium for 24 h. Spot Western blot analysis of extracts demonstrated the presence of the expected *c-myc*-tagged proteins in each extract (Fig. 3). Overexpression of either Bgs13-*c-myc*-His₆ (pKdSC5) or Remi-bgs13-*c-myc*-His₆ (pAH1) did not affect the growth rate of either strain, compared to a negative-control strain that harbored an empty plasmid (data not shown). For reasons that were not clear, however, we were unable to isolate either wt Bgs13-*c-myc*-His₆ or Remi-bgs13-*c-myc*-His₆ from these extracts, using both nickel and cobalt affinity columns. Thus, to try to compare specific activity, spot Western blot analysis was used to determine volumes of extracts with equal levels of the wt Bgs13-*c-myc*-His₆ and Remi-bgs13-*c-myc*-His₆ peptides. These volumes were then assayed for PKC activity. Our results indicated that the Remi-bgs13-*c-myc*-His₆ protein had much lower PKC specific activity than did the wt Bgs13-*c-myc*-His₆ peptide (Table 1).

This result led to the initial hypothesis that improved secretion of the *bgs13* strain resulted from a decrease in PKC activity. We reasoned that if this were true, then elevated levels of PKC activity would decrease the secretion of a reporter. We chose human secretory leukocyte protease inhibitor protein (SLPI) as the recombinant reporter because it is a secreted human protein, containing eight disulfide bonds, that had been shown previously by our laboratory to be secreted at higher levels by our *bgs13* strain than by the wt parent strain (7, 23). Therefore, a strain that expressed SLPI under the control of the *AOX1* promoter was transformed with a plasmid that overexpressed the wt Bgs13-*c-myc*-His₆ peptide (pKdSC5) or an empty plasmid. As shown in

TABLE 1 PKC activity of extracts^a

Sample	PKC activity ($\Delta A_{450}/\text{min}/\text{mg}$ total protein)
Kit	
Positive control, 1 \times	0.318
Positive control, 1/2 \times	0.195
Extract	
Bgs13- <i>c-myc</i> -His ₆	0.174
REMI-bgs13- <i>c-myc</i> -His ₆	0.106
Negative control	0.084

^aCytoplasmic extracts were isolated from strains that expressed either Bgs13p variant from the *AOX1* promoter. Cells were grown in dextrose, induced with methanol for 24 h, and harvested. Equivalent amounts of Bgs13-*c-myc*-His₆ and REMI-bgs13-*c-myc*-His₆ were used in assays with a PKC activity kit (Enzo Life Sciences). The negative control was an extract made from a wt strain containing an empty pPICZB plasmid. The values represent averages of two runs.

TABLE 2 Secreted levels of SLPI protein in strains producing normal (yAM1-pPICZB) or elevated (yAM1-pKdSC5) levels of Bgs13p

Strain	Time of induction (h)	Secreted SLPI protein level (% of wt value)
yAM1-pPICZB	48	100.00
yAM1-pKdSC5	48	59.31
yAM1-pPICZB	72	100.00
yAM1-pKdSC5	72	55.05

Table 2, overexpression of Bgs13p reduced secretion of SLPI by approximately 50%, compared to a strain with normal levels of endogenous Bgs13p. It could be argued that the reduction in SLPI secretion was due to the secretory stress created by the addition of an *AOX1* promoter-*BGS13* expression construct to a strain that already contained an *AOX1* promoter-*SLPI* expression cassette. However, a previously published report (23) from our laboratory demonstrated that a strain carrying two copies of an *AOX1p-SLPI* expression cassette secreted approximately twice as much SLPI peptide as a strain harboring a single copy of this expression cassette. This finding supported our hypothesis that the secretion efficiency of a strain may be inversely proportional to its PKC activity.

Determining the localization of Bgs13p. Although these experiments suggested that secretion levels were regulated by the PKC activity of Remi-bgs13p, we also wanted to determine whether the localization of Remi-bgs13p played a role in modulating the levels of recombinant protein secretion. Because deletion of the HR1 domains in *S. cerevisiae* Pkc1p affected its cellular location (15), we attempted to determine whether there was a difference in the cellular locations of Bgs13p and Remi-bgs13p. To pursue this idea, an N-terminal wt Bgs13p or Remi-Bgs13p sequence was fused to a C-terminal EGFP sequence and expressed in wt cells. Fluorescence microscopy was subsequently employed to determine the location of the fusion proteins, using FM 4-64 dye [*N*-(3-triethylammoniumpropyl)-4-(6-[4-(diethylamino)phenyl]hexatrienyl)pyridinium dibromide] to stain the vacuole as a reference point in the *P. pastoris* cells (12). While the wt Bgs13-EGFP peptide was concentrated near the neck and bud of dividing cells, the mutant protein-EGFP fusion was found on the periphery of the cell (Fig. 4). The observation that the two Bgs13p forms were localized to different regions of the cell suggests that, potentially, the peptides were able to interact with different molecular partners in the cell. Interestingly, wt Bgs13p showed localization similar to that of *S. cerevisiae* wt Pkc1p; however, deletion of the N-terminal

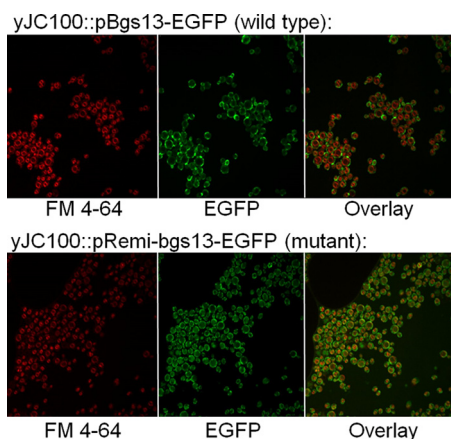


FIG 4 Confocal fluorescence images of Bgs13-EGFP and Remi-bgs13-EGFP fusions. Strains expressing Bgs13-EGFP and Remi-bgs13 fusions from the *AOX1* promoter were grown on glycerol and then induced on methanol-containing medium. These cells were then subjected to confocal fluorescence microscopy to detect EGFP, and the vacuolar membranes were stained with FM 4-64. The images were subsequently merged.

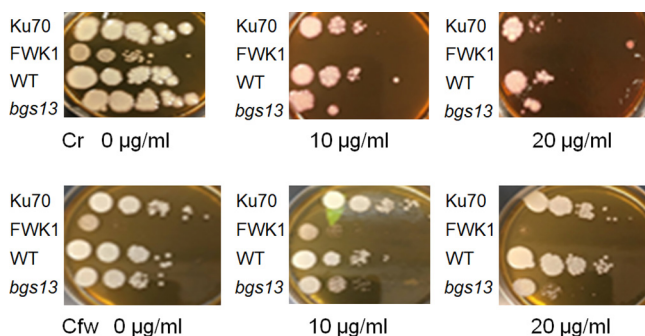


FIG 5 Sensitivity of *bgs13* cell walls to Cr and Cfw. The indicated strains were grown to mid-log phase (OD_{600} values of 5 to 10) on YPD medium. Cell densities were normalized to an OD_{600} of 1.0 and diluted four times in a 10-fold series (10^0 , 10^{-1} , 10^{-2} , 10^{-3} , and 10^{-4}). Equal volumes of each dilution were spotted on YPD plates containing the indicated concentrations of either Cr or Cfw. The plates were incubated at 30°C for 3 to 4 days and photographed.

region of Pkc1p caused it to be relocated to the nucleus in baker's yeast, not to the cell periphery as seen in *P. pastoris* (15). Furthermore, the kinase activity of Pkc1p was found to be necessary for its localization to the bud neck region; a 1-amino-acid substitution in the kinase domain that reduced activity caused mislocalization. For Remi-*bgs13p*, the different localization might have changed its molecular partners, which in turn reduced activity, or its reduced activity interfered with its normal localization. Overall, the substitution of the first 147 amino acids of the Bgs13p with 12 amino acids in Remi-*bgs13p* caused changes in its cellular location and PKC activity, either or both of which may ultimately result in enhanced secretion.

Characterization of the structural defects of the *bgs13* strain cell wall. Having focused on the properties of the wt strain and the mutant Bgs13ps strain, we next turned our attention to the downstream effects of Remi-*bgs13p*, compared to its wt counterpart. Because of *S. cerevisiae* Pkc1p involvement in CWI, we first focused on examining the influence of Remi-*bgs13p* on the cell wall. In our first test, Congo red (Cr) and Calcofluor white (Cfw) were used to detect any cell wall defects in the wt and *bgs13* strains. Both compounds are thought to interfere with cell wall assembly by binding to chitin in *S. cerevisiae* (24). The more chitin that is present, the greater is the binding of Cr and Cfw and thus the more severe is the weakening of the cell wall structure. In response to cell wall stress, yeast cell wall chitin levels can increase to as much as 20% of total wall polymer (10). Most cell wall mutants, such as those with disturbances in the synthesis of 1,3- β -glucan or the mannosylation of proteins, have more chitin in their cell walls than wt strain cells and thus are more sensitive to both Cfw and Cr (24). Before determining the sensitivity of our *bgs13* strain, we confirmed that the FWK1 strain, a *P. pastoris* $\Delta och1$ strain with a deletion in a mannosyltransferase gene and a well characterized cell wall defect (25), showed decreased colony density with increasing levels of both Cr and Cfw, compared to its wt parent Ku70 (Fig. 5). In the same manner, the *bgs13* strain displayed cell wall defects demonstrated by greater sensitivity to these compounds, compared to its parent strain. Furthermore, transmission electron microscopy showed that *bgs13* strain cells contained a thicker cell wall than wt parent cells (Fig. 6), another indication that a cell wall defect is present (26). These results were consistent with our previous finding that the *bgs13* strain released higher levels of alkaline phosphatase than the wt strain, which was also interpreted as a sign of a cell wall weakness (7). Furthermore, in the previous work, the addition of the osmotic stabilizer sorbitol decreased alkaline phosphatase release into the ECM, strongly suggesting that CWI is compromised by the Remi-*bgs13p* function.

Determining the effect of DTT on cell wall proteins. To delve further into this question and to examine the structure of the cell walls of the wt and mutant strain cells, we performed a dithiothreitol (DTT) extraction analysis. DTT liberates noncovalently and dithiol-linked cell wall proteins, yielding increased amounts of extractable proteins

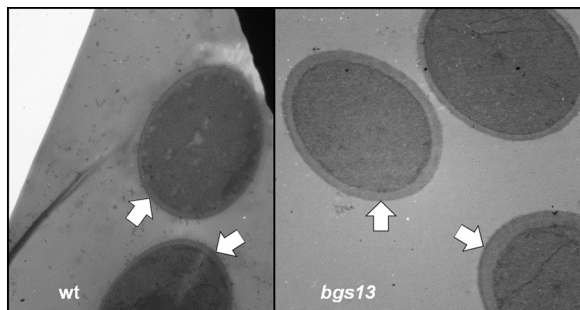


FIG 6 Transmission electron microscopy of wt strain and *bgs13* strain cells. Both wt strain and *bgs13* strain cells were grown in YPD medium, and electron micrographs were taken at $\times 12,000$ magnification. Arrows indicate the cell walls.

when the cell wall is defective (27). It is expected that defects in the cell wall composition or structure would lead to increases in DTT-extractable proteins. Treatment of equivalent numbers of wt and *bgs13* strain cells with DTT demonstrated that the mutant strain had higher levels (approximately 2- to 3-fold higher) of DTT-extractable proteins, as detected by SDS-PAGE with silver staining (Fig. 7). Novel protein bands appeared to be released from the *bgs13* strain cell walls, while other protein bands seemed to become more prominent, especially those at 40 to 45 kDa; this was true for the strain grown on both simple and enriched methanol-based media.

Measurement of cell wall porosity. However, two pieces of evidence seemed to contradict the hypothesis that a weakened cell wall was the cause of increased secretion (28). First, if a weakened cell wall were responsible for allowing greater protein secretion, then sorbitol addition should decrease secretion of a reporter such as SLPI. However, the addition of sorbitol to the *bgs13* strain, which used a *GAP* promoter to constitutively secrete a SLPI reporter, did not reduce secretion as expected but actually increased export into the ECM (data not shown). Second, hypersensitivities to Cfw and Cr are associated with a more porous cell wall (25). A more porous cell wall could be expected to be more permeable to proteins delivered outside the plasma membrane by the secretory system, allowing entry into the ECM. To measure cell wall porosity, both wt and *bgs13* strain cells were exposed to DEAE-dextran, which has a large hydrodynamic radius, and poly-L-lysine, which has a small hydrodynamic radius.

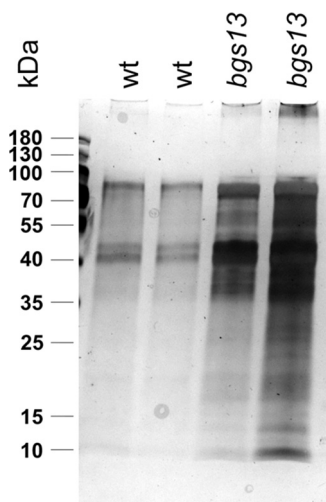


FIG 7 SDS-PAGE analysis of proteins extracted from the cell wall. Two samples (each) of wild-type and *bgs13* strain cells were grown on glucose, induced on BMM, and harvested. After washing, the cells were subjected to DTT treatment to extract proteins from the cell wall. A silver stain analysis of proteins separated by SDS-PAGE was then performed.

TABLE 3 Relative cell wall porosity, as determined by a polycationic assay^a

Strain	Relative cell wall porosity (%)
Wild-type strain	31.9 ± 3.11
<i>bgs13</i> strain	22.4 ± 2.92
Ku70	12.2 ± 4.94
FWK1	122 ± 14.0

^aA strain (FWK1) with a known cell wall defect caused by deletion of the *OCH1* gene and its parent strain (Ku70) were analyzed for comparison. Data reflect the averages of duplicates.

While DEAE-dextran can damage the plasma membrane and release nucleic acids only if sufficiently large pores exist in the cell wall, poly-L-lysine constitutively causes cell leakage and nucleic acid release (25, 29). Therefore, by measuring the UV-absorbing compounds released from the cells by DEAE-dextran versus poly-L-lysine, the relative cell wall porosity can be determined. To ensure that the assay was being performed correctly, we measured the relative cell wall porosity of a $\Delta och1$ strain of *P. pastoris* and its wt parent. The $\Delta och1$ strain of *Saccharomyces cerevisiae*, which lacks a Golgi mannosyltransferase, has been demonstrated to have increased cell wall porosity, compared to its parent (25). After confirming that the *P. pastoris* $\Delta och1$ strain showed the same phenotype, we found that the *bgs13* mutant actually had a cell wall with slightly less porosity than its wt parent (Table 3). Thus, the *bgs13* strain contains a cell wall with structural defects that make it more sensitive to Cfw and Cr but with less porosity than the wt cell wall, in contrast to findings observed for the *P. pastoris* $\Delta och1$ strain, which showed structural anomalies and greater porosity. Moreover, a previous study demonstrated that the *P. pastoris* $\Delta och1$ strain actually displayed a 30% reduction in the export of horseradish peroxidase (30). This finding suggests that any impact of cell wall porosity on secretion of a specific polypeptide depends on the unique properties of that protein. Thus, the combination of these results complicates the simple conclusion that a defective cell wall led to greater permeability, which in turn increased protein export.

ESI-MS/MS analyses of proteins in the ECM of wt and *bgs13* strains. Because the *bgs13* mutation resulted in different proteins being deposited in the cell wall and these proteins travelled through the secretory organelles of the yeast before reaching this destination (26), we wished to extend our analysis to the proteins delivered by the secretory pathway (i) into the ECM and (ii) to the cell wall of both wt and mutant strains. Previous experiments increased the secretion of four of five reporter proteins in the *bgs13* strain (7). Thus, our first approach was to use electrospray ionization (ESI)-mass spectrometry to compare the entire populations of proteins secreted by the wt and mutant strains. Through a label-free quantitative approach, we analyzed equal amounts of proteins in the strains' ECM and spiked the samples with equivalent amounts of bovine serum albumin (BSA) and myoglobin. To identify the proteins present and to quantitate their relative abundance in the shake flask culture medium from both mutant *bgs13* and wt strains, the strains were induced with methanol, and the peptides were collected, solubilized in 3 M urea, and subjected to overnight digestion with trypsin. The tryptic peptides were then separated via nano-liquid chromatography, eluted, and ionized by ESI for tandem mass spectrometry (MS/MS) analysis. Within both wt strain ECM and mutant *bgs13* strain ECM, a total of 337 proteins were identified with high levels of confidence (>2 unique peptides mapping back to each identified protein across all six technical replicates). The relative abundance of the 335 identified proteins found in the postinduction ECM was calculated as the ratio of the protein's grouped (i.e., average) abundance in the *bgs13* strain ECM to the protein's grouped abundance in the wt strain ECM. Fold changes in the abundance of proteins were calculated with the \log_2 (abundance ratio), which was subsequently displayed in a volcano plot (Fig. 8). The volcano plot displays fold changes versus significance (on the x and y axes, respectively), resulting in data points with low *P* values (highly significant) appearing toward the top of the plot. Therefore, proteins with the greatest increase in relative

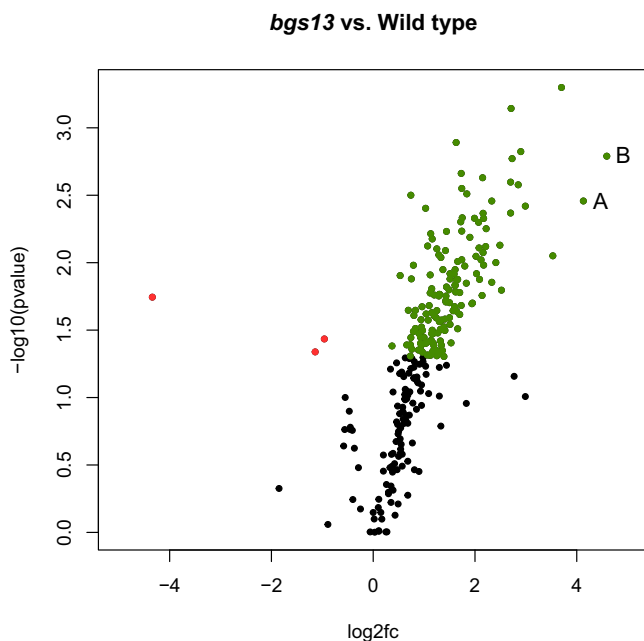


FIG 8 Differential protein populations found in the ECM of shake flask cultures grown at 28°C. A volcano plot illustrates the differential abundance of proteins found in the ECM of wt and *bgs13* strain cells expressing the MBP-EGFP reporter. Differentially abundant proteins of statistical significance ($P \leq 0.05$) are shown in red (wt strain) and green (*bgs13* mutant); x axis, \log_2 (fold change), i.e., fold change in abundance between the two populations (wt strain and *bgs13* mutant); y axis, $-\log_{10}(P)$, i.e., statistical significance of the fold change in abundance. Fold changes were calculated as \log_2 (abundance ratio) (*bgs13* strain/wt strain); for the three technical replicates for each strain, the abundance of each identified protein was grouped (averaged) for use in the abundance ratio and fold change analyses. “A” represents MBP, while “B” represents EGFP.

abundance in the *bgs13* strain secreted fraction and with high significance are found in the top right portion of the graph.

Both the wt and *bgs13* strains depicted in the volcano plot were engineered to secrete a fusion of MBP and EGFP under methanol growth conditions, the export of which was studied previously (12). The fusion was proteolyzed into its two domains prior to secretion. As demonstrated in a Western blot analysis (Fig. 9), the *bgs13* strain secreted about 20 times as much MBP-EGFP as its parent strain, according to densitometry analysis. The MBP from MBP-EGFP is slightly larger than the positive-control MBP purified from bacteria because it contains a few extra amino acids from a linker region located between the MBP and EGFP domains. Consistent with the Western blot data, the volcano plot indicated that MBP (indicated by an A) and EGFP (indicated by a B) were found to have abundance ratios of 17.52 and 24.04, respectively, validating the relevance of our analysis (Fig. 8).

Overall, the secretome analysis demonstrated that, of the proteins released by both strains, most were released at significantly higher levels by the *bgs13* strain. Through manual annotation of the protein hits provided by Proteome Discoverer 2.2, nine previously characterized proteins that are secreted or contain a signal peptide sequence were identified (Table 4). These proteins included cell wall-associated proteins such as 1,3- β -glucanoyltransferase (ATY40_BA7501626) and exo-1,3- β -glucanase (*EXG*), as well as other native proteins such as vacuolar proteases (BA75_01312T0 [*PRB1*] and BA75_03408T0 [*PEP4*]). Extracellular protein X1 (Epx1) (BA75_03408T0 [*PRY2*]) is one of the most abundantly secreted proteins in chemostat cultures of wt *P. pastoris* and is considered a major contaminant during the purification of recombinant proteins (57). If Epx1 export was increased by the *bgs13* mutation, this would have worsened an already difficult problem. However, Epx1 was found at equal levels (abundance ratio of 1.014) in the ECM of both *bgs13* and wt strains. Thus, the *bgs13* mutation does not

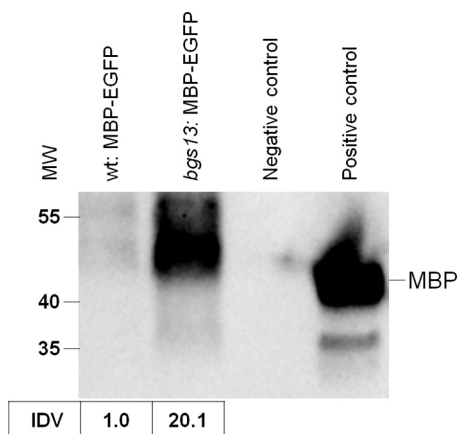


FIG 9 Western blot analysis of extracellular fractions from strains expressing MBP-EGFP. Wild-type and *bgs13* strains containing an MBP-EGFP fusion and a wt strain containing an empty plasmid, pPICZαB (negative control), were grown on glycerol-containing medium to accumulate biomass, induced on methanol-containing medium to express recombinant protein, and pelleted. Volumes of extracellular supernatants, corresponding to equivalent numbers of cells (based on OD₆₀₀ values), were probed with anti-MBP antibody. Fifty nanograms of commercially available MBP was used as a positive control. Images were captured with a Chemilmager 5500 and quantified with IDV analysis.

increase the secretion of a major contaminant, which is an attractive aspect of the *bgs13* mutant strain.

Furthermore, of the 335 proteins that were identified in the ECM of both strains, many intracellular proteins were found, most likely due to cell lysis of older cells, which was noted in a previous proteomic analysis of a wt *P. pastoris* secretome (31). A defective cell wall would make the *bgs13* strain cells more susceptible to cell lysis. Cell wall defects have been demonstrated to arise from perturbations in the CWI pathway, which has been shown to be coordinated regulated with the unfolded protein response (UPR) (10, 32). Sensitivity to Cr and Cfw, increased levels of DTT-extractable cell wall proteins, and enhanced secretion of some recombinant proteins are phenotypes of cells with a disrupted UPR. The UPR is an endoplasmic reticulum (ER)-to-nucleus signaling pathway initiated by ER stress, such as the buildup of unfolded proteins in the ER that can result from protein overexpression (33–35). The UPR attempts to reduce this ER stress by activating a large number of target genes, whose products function in a range of activities, such as enhanced protein folding to improve secretion efficiency and protein degradation to remove unfolded aggregate peptides. The combined actions of these UPR mechanisms should ultimately reduce the buildup of unfolded proteins in the secretory mechanism. Thus, it could be hypothesized that Remi-*bgs13*p triggers abnormal UPR activity, which leads to greater secretion in addition to a weaker cell wall.

TABLE 4 Summary of information on identified representative proteins in the ECM that contained a signal peptide sequence

UniProt accession no.	Protein name	Gene name	Description	Abundance ratio (<i>bgs13</i> strain/wt strain)
A0A1B2J7P6	1,3-β-Glucanosyltransferase	ATY40_BA7501626 (<i>K. pastoris</i>) ^a	Involved in cell wall biosynthesis and morphogenesis	4.268
A0A1B2JAX4	BA75_02022T0	ATY40_BA7502022 (<i>K. pastoris</i>)	Cell wall protein with putative GPI attachment site ^b	2.840
A0A1B2JF94	BA75_03408T0	PEP4 (<i>K. pastoris</i>)	Vacuolar aspartyl protease (proteinase A)	1.472
Q2TCV2	Exo-1,3-β-Glucanase	EXG (<i>K. pastoris</i>)	Involved in cell wall β-glucan assembly and maintenance	1.306
A0A1B2J758	BA75_01312T0	PRB1 (<i>K. pastoris</i>)	Vacuolar proteinase B (YscB), serine protease of subtilisin family	1.075
A0A1B2J5U4	BA75_00070T0	PRY2 (<i>K. pastoris</i>)	Sterol-binding protein involved in export of acetylated sterols	1.014
A0A1B2J755	BA75_01624T0	ATY40_BA7501624 (<i>K. pastoris</i>)	Cell wall protein with similarity to glucanases	0.728
A0A1B2JDU3	BA75_03273T0	ATY40_BA7503273 (<i>K. pastoris</i>)	Mitochondrial outer membrane and cell wall localized SUN family member	0.724
A0A1B2JDF4	BA75_02994T0	YDR262W (<i>K. pastoris</i>)	Putative protein of unknown function	0.667

^a*Komagataella pastoris* is the reassigned name for *Pichia pastoris* and is used by the UniProt/Swiss-Prot database.

^bGPI, glycosylphosphatidylinositol.

The differentially abundant intracellular proteins also included those associated with the UPR mechanism (the ER chaperones BiP [*KAR2*] and protein disulfide isomerase [*PDI*]) and others involved in protein folding and aggregation (BA75_00603T0 [*CPR6*], BA75_00961T0 [*SGT2*], BA75_01760T0 [*HSP104*], BA75_02652T0 [*STI1*], BA75_00236T0, and ATY40_BA7500236) (see Fig. S1 in the supplemental material). Three pieces of evidence connect the *bgs13* strain to a change in the UPR. First, the overexpression of the Hac1 protein, a master transcriptional activator of UPR genes, causes the secretion of Kar2/BiP, protein disulfide isomerase (PDI), and other chaperone-type proteins (containing the HDEL retention sequence) into the ECM, possibly because the capacity of the ER retrieval mechanism is exceeded when the UPR is induced (36). Second, Kar2p/BiP and PDI were found in the ECM when recombinant secretory insulin precursor secretion triggered the UPR in another study (37). Lastly, Yu et al., when comparing the transcriptomes of recombinant strains containing either 12 copies or single copies of a bacterial phospholipase gene, identified the most significant, differentially expressed genes found at higher levels in the multicopy strain, which were involved in ER protein processing and heat shock responses (38). Of the eight top genes, six were found in greater abundance in the *bgs13* strain than in the wt strain (Fig. S1). These similarities suggest that Bgs13p may be involved in the UPR mechanism and the lack of the first 147 amino acids in Remi-bgs13p may affect normal UPR activity. Thus, the *bgs13* mutation has a global effect on the secretory mechanism, influencing the export of a diverse array of proteins, with links to the CWI and UPR.

ESI-MS/MS analyses of proteins in the cell wall of wt and *bgs13* strains. The increased amounts of ECM proteins from the *bgs13* strain cells justified the use of the DTT-extracted cell wall proteins as the next protein population for mass spectrometry analysis. After removal of all traces of ECM, the protein populations were extracted from the cell walls of both the wt strain and the mutant *bgs13* strain (Fig. 7) and underwent sample preparation, tryptic digestion, and subsequent data analysis. A total of 359 proteins were identified with high confidence in the cell wall extracts from both strains, with 23 proteins being classified as either uncharacterized or hypothetical proteins. The fold changes in the differential abundance of the 359 proteins are graphically represented in a volcano plot in Fig. 10. Similar to those found in the ECM, the majority of the proteins were more abundant in the mutant *bgs13* strain cells than in the wt strain cells (Fig. S2). The recombinant reporter proteins EGFP and MBP were found to be more abundant in the *bgs13* strain (abundance ratios of 2.262 and 1.977, respectively). These proteins may be present either because of being retained inside the cell wall during transit to the ECM or because of being released by cell lysis.

Through manual annotation of the protein hits provided by Proteome Discoverer 2.2, eight previously characterized cell wall-associated proteins were identified, including multiple isoforms of 1,3- β -glucanase, an endo-1,3- β -glucanase, and a putative aspartic protease (Table 5). Two of the 1,3- β -glucanase isoforms, encoded by ATY40_BA7501626 and *GAS1*, were the only characterized cell wall-associated proteins that displayed greater abundance in the *bgs13* strain extract. Surprisingly, most of the cell wall-associated peptides were found in greater abundance in the wt strain; the reason for this is unclear. In *S. cerevisiae*, the Pkc1 kinase in the CWI pathway represses some enzymes involved in the biosynthesis and assembly of the cell wall, including β -glucanase encoded by *BGL2* (39). In *S. cerevisiae* Δ *pkc1* strain cells, overproduction of β -glucanase was partially responsible for a weakened cell wall and a growth defect. It is possible that a similar scenario is occurring in the *bgs13* strain of *P. pastoris*; the hybrid Remi-bgs13p may be affecting the regulation of specific cell wall-associated proteins.

Furthermore, many of the 359 cell wall-extracted proteins were of intracellular origin, such as key proteins involved in the UPR and protein folding, including PDI (abundance ratio of 1.70) and BiP/Kar2p (abundance ratio of 2.292), just as in the ECM. Their presence in the cell wall extract could suggest that Remi-bgs13p leads to either (i) inefficient retention of these ER-resident proteins, leading to mistargeting and

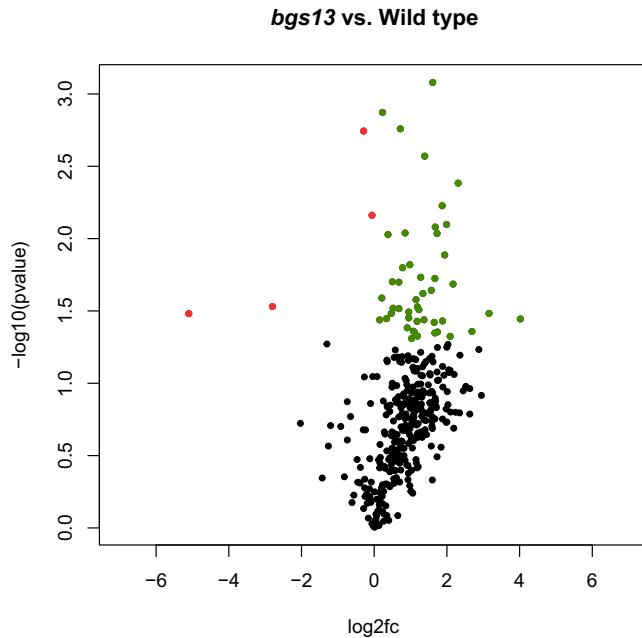


FIG 10 Differential protein populations identified from DTT extraction of the cell wall from cells grown in shake flask cultures at 28°C. A volcano plot illustrates the differential abundance of proteins extracted from the cell walls of wt and *bgs13* strain cells after methanol induction, as shown in Fig. 8. Differentially abundant proteins of statistical significance ($P \leq 0.05$) are shown in red (wt strain) and green (*bgs13* mutant); x axis, $\log_2(\text{fold change})$, i.e., fold change in abundance between the two populations (wt strain and *bgs13* mutant); y axis, $-\log_{10}(P)$, i.e., statistical significance of the fold change in abundance. Fold changes were calculated by taking the $\log_2(\text{abundance ratio})$ (*bgs13* strain/wt strain); for the three technical replicates for each strain, the abundance of each identified protein was grouped (averaged) for use in the abundance ratio and fold change analyses.

incorporation into the cell wall, with liberation by DTT, or (ii) lysis due to a weakened cell wall, leading to the release of chaperones into the extract.

Quantitation of intracellular PDI expression. To help differentiate between these two possibilities, we quantified the intracellular levels of PDI. We hypothesized that, if Remi-*bgs13p* caused PDI to be overexpressed, not retrieved efficiently, and allowed to enter the cell wall and ECM, then the intracellular levels of PDI should be roughly the same inside wt strain cells and mutant cells. However, if PDI was overexpressed, accumulated inside the ER, and was released only after cell lysis, then the levels of PDI would be much higher inside *bgs13* strain cells, relative to wt strain cells. To quantitate intracellular PDI levels, proteins were extracted from equal numbers of mutant and wt cells and separated into soluble/cytoplasmic and insoluble/membrane-associated fractions. PDI is usually found in an insoluble membrane fraction of *P. pastoris* cells (40, 41).

TABLE 5 Summary of information on identified representative cell wall-associated proteins from DTT extraction of the cell wall

UniProt accession no.	Protein name	Gene name	Description	Abundance ratio (<i>bgs13</i> strain/wt strain)
A0A1B2JAX4	BA75_02022T0	ATY40_BA7502022 (<i>K. pastoris</i>) ^a	Cell wall protein with putative GPI attachment site ^b	4.073
A0A1B2J7P6	1,3-β-Glucanoyltransferase	ATY40_BA7501626 (<i>K. pastoris</i>)	Involved in cell wall biosynthesis and morphogenesis	3.710
A0A1B2J5A4	1,3-β-Glucanoyltransferase	<i>GAS1</i> (<i>K. pastoris</i>)	Involved in cell wall biosynthesis and morphogenesis	1.629
A0A1B2J7D2	BA75_00420T0	<i>YPS7</i> (<i>K. pastoris</i>)	Putative GPI-anchored aspartic protease; involved in cell wall growth and maintenance	0.940
A0A1B2JJE0	BA75_04772T0	ATY40_BA7504772 (<i>K. pastoris</i>)	Chitin transglycosylase	0.721
A0A1B2J755	BA75_01624T0	ATY40_BA7501624 (<i>K. pastoris</i>)	Cell wall protein with similarity to glucanases	0.657
A0A1B2JGR3	1,3-β-Glucanoyltransferase	<i>GAS3</i> (<i>K. pastoris</i>)	Involved in cell wall biosynthesis and morphogenesis	0.418
A0A1B2JF97	BA75_03970T0	<i>BGL2</i> (<i>K. pastoris</i>)	Endo-β-1,3-glucanase involved in incorporation of newly synthesized mannoprotein into cell wall	0.406

^a*Komagataella pastoris* is the reassigned name for *Pichia pastoris* and is used by the UniProt/Swiss-Prot database.

^bGPI, glycosylphosphatidylinositol.

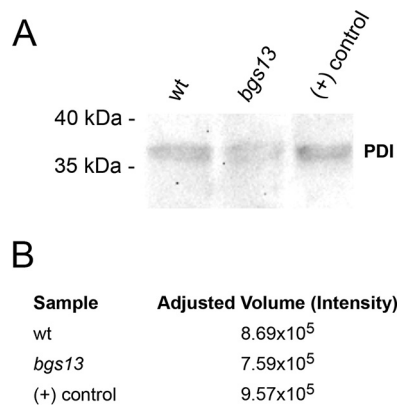


FIG 11 Intracellular PDI expression levels in *P. pastoris* strains after methanol-induced recombinant protein expression. (A) Immunoblot analysis of intracellular PDI levels extracted from insoluble membrane-associated fractions. The strains, which expressed the human SLPI protein, were grown on glucose, induced with methanol, and harvested. Insoluble membrane-associated fractions were isolated from the cell pellets, and equal amounts of protein were probed with an anti-PDI antibody. The positive control overexpressed PDI from the *AOX1* promoter. (B) Quantitation of the intensity of each strain's detected PDI with IDV analysis.

Equal amounts of protein from each strain's soluble and insoluble fractions were subjected to Western blot analysis with a primary antibody against PDI (Fig. 11A). In addition, a strain overexpressing PDI from the *AOX1* promoter was utilized as a positive control (23). In our immunoblots, the PDI overexpression strain contained about 20% more detectable PDI than these strains (Fig. 11B), which was consistent with previous results (23). Furthermore, our Western blot analysis indicated that, while PDI was undetectable in the soluble fraction of each strain, approximately equal amounts of the chaperone were detected in the insoluble membrane fractions of both mutant and wt cells. Taken together, these results suggest that, if PDI is overproduced due to the *bgs13* mutation, then it saturates the capacity of the ER and proceeds through the secretory system, arriving at the cell wall and ECM. Thus, in the context of previous findings regarding the *bgs13* strain, our work demonstrates that Remi-*bgs13*p changes the protein-sorting mechanism and leads to changes in protein localization in *P. pastoris* cells.

Conclusions. The insertion of the pREMI plasmid into the *BGS13* locus created a gene that expressed a Bgs13p lacking its first 147 amino acids. This mutant version had lower PKC activity and was localized to a different cellular region, compared to its wt counterpart. Because overexpression of wt Bgs13p decreased the secretion of a SLPI reporter, we think that the decreased PKC activity found for Remi-*bgs13*p was at least partially responsible for increases in the secretion levels of multiple reporters (including MBP-EGFP), as well as native proteins, as revealed by mass spectrometry analysis. The reduction in kinase activity would justify an examination of the members of the MAPK cascade in the CWI pathway. However, certain proteins were secreted at the same levels in the wt and *bgs13* strains, indicating that the mutation did not have a universal effect.

One salient effect of this enhanced protein export was a defect in cell wall construction, since the *bgs13* strain cell wall not only became more sensitive to Cr and Cfw but also released greater amounts of protein when subjected to DTT extraction. These effects are also seen in *S. cerevisiae* cells with a decreased UPR (27) but, unlike that strain, the *P. pastoris bgs13* mutant did not display increased porosity of the cell wall or a thinner cell wall. However, the *bgs13* strain demonstrated overexpression of BiP and PDI, an effect seen in *P. pastoris* strains with elevated Hac1p levels and increased UPR (36). In the *bgs13* strain, PDI was present in the cell wall and ECM, suggesting a difference in protein sorting. Coupled with this result is the previous finding (12) that the *bgs13* allele caused MBP-EGFP to be shunted from the vacuole (its normal destination in the wt strain) and localized to other parts of the secretory network prior to its

export into the ECM. Taken together, these results suggest that the *bgs13* strain is a supersecretor not because it has a more porous cell wall but because its novel protein-sorting mechanism causes a large increase in the secretion of proteins, which results in an altered composition and structure of its cell wall.

The *bgs13* strain has several similarities and differences with respect to cells with decreased UPR. Thus, Remi-*bgs13p* does not simply activate or deactivate the UPR. The UPR has two major mechanisms to ameliorate the ER stress brought on by protein buildup in secretory organelles associated with high levels of recombinant peptide expression, namely, the degradation of misfolded proteins and the enhanced folding of nascent peptides (33). In our current model, Remi-*bgs13p* may be influencing these two mechanisms by either (i) downregulating the UPR, which causes misfolded and/or incorrectly modified proteins to circumvent vacuolar targeting and allows them to enter the cell wall or ECM (it has been suggested that defects in cell wall structure may stem from the incorporation of misprocessed and/or misfolded proteins in the cell wall [32, 42]), or (ii) upregulating the UPR, which leads to an increase in folding with high fidelity and allows more correctly proteins to be successfully secreted. Our future experiments will determine which model is correct by using mass spectrometry to examine the folding of proteins that show enhanced secretion. Using matrix-assisted laser desorption–time of flight mass spectrometry, the differences in disulfide linkages of the reporter protein SLPI produced in the wt strain versus the *bgs13* strain can be elucidated. Thus, differences in disulfide linkages will give information about the protein-folding capabilities of the two strains. Understanding this critical step in how Bgs13p modification leads to supersecretion not only will shed light on the basic principles of protein export but also could lead to new approaches to make *P. pastoris* a better recombinant host system.

MATERIALS AND METHODS

Strains and growth conditions. *Escherichia coli* One Shot TOP10 chemically competent cells (Life Technologies, Carlsbad, CA) were used for transformation and plasmid DNA amplification unless stated otherwise. The TOP10 transformants were grown at 37°C in Lennox broth (LB) with the addition of 100 µg/ml ampicillin or 25 µg/ml Zeocin, in a New Brunswick Scientific C25 incubating shaker (New Brunswick Scientific Edison, NJ) at 225 rpm. The *P. pastoris* wt strain, yJC100, was derived from the original strain NRRL Y11430 (North Regional Research Laboratories, US Department of Agriculture, Peoria, IL). The yDT39 strain (*his4 met2*) (43) and the *bgs13* mutant (7) derived from it were generated in our laboratory. These yeast strains were cultured in YPD medium (1% yeast extract, 2% peptone, 2% glucose) supplemented with 100 µg/ml Zeocin or 0.5 mg/ml G418 for antibiotic resistance selection, YND medium (0.17% yeast nitrogen base [YNB] with 0.5% ammonium sulfate and 0.4% glucose), basic medium with glucose and YNB (BMGY) (1% glycerol, 2% peptone, 2% glucose, 1.34% YNB, 0.00004% biotin, 100 mM potassium phosphate [pH 6.0]), or basic medium with methanol and YNB (BMMY) (0.5% methanol, 2% peptone, 1% yeast extract, 1.34% YNB, 0.00004% biotin, 100 mM potassium phosphate [pH 6.0]) (44). *P. pastoris* cells were grown in liquid culture at 28°C in a shaking incubator (model 1585; VWR, Batavia, IL) set to 325 rpm, while cells that were grown on agar plates were incubated at 30°C in a Fisher Scientific Isotemp incubator (Fisher Scientific, Pittsburgh, PA). Optical density at 600 nm (OD_{600}) values were measured using a Spectronic Genesys 2 spectrophotometer (Spectronic Instruments Inc., Rochester, NY).

Recombinant DNA procedures, including bacterial transformation, were performed essentially as described previously (45). Plasmid DNA was purified from *E. coli* cultures using a QIAprep Spin miniprep kit (Qiagen, Chatsworth, CA). Linear plasmid DNA and PCR products were cleaned and concentrated using the Zippy DNA Clean and Concentrator kit (Zymo Research, Irvine, CA). Restriction enzymes were purchased from MBI Fermentas (Hanover, MD). Precast 1.2% agarose Flash gels (Lonza, Rockland, ME) were used to analyze the restriction digestion products. Oligonucleotides were synthesized by Sigma Genosys (Plano, TX). All mutated sites and ligation junctions in newly synthesized vectors were confirmed by DNA sequencing (Quintara Biosciences, South San Francisco, CA). The CRISPR *BGS13* knockout plasmids were kindly provided by Anton Glieder (Technical University of Graz). The MBP used as a positive control in Western blot analyses was purchased from New England Biolabs (Ipswich, MA). DNA concentrations were determined using a NanoDrop 2000c spectrophotometer (Thermo Fisher Scientific) set to 260 nm. Sequence analyses were performed with SnapGene software (GSL Biotech, Chicago, IL).

PCR analysis of cDNA from the *bgs13* strain. Wild-type and *bgs13* strain cells were grown as described below (in “Large-Scale Expression”) but the cell pellets were harvested after a 24-h methanol induction, washed with diethyl pyrocarbonate (DEPC)-treated water, and frozen at –80°C. Total RNA was isolated from both cell types by a standard procedure adapted for total yeast RNA isolation (46). After incubation with RNase-free DNase, the RNA was reverse transcribed from approximately 1 µg of total RNA using the ProtoScript first-strand cDNA synthesis kit (New England BioLabs, Ipswich, MA), according to the manufacturer’s instructions. Two microliters of the cDNA product was then subjected to standard PCR using the primers TTGATCCCATACTGGCAATTGTGTGC and TTGAGCTCGGTCGCGTAAGAAT

GGA, to determine whether the 3' end of *BGS13* was present in the wt and *Remi-bgs13* transcripts (expected 650-bp product). The same PCR procedure was performed with cDNA product template primers GAGGTAC CTGTGACAGACAAGCAATGATGA and AAAGCCATCTTCATCAAATG, to determine whether the 5' end of *BGS13* was present in the wt and *Remi-bgs13* transcripts (expected 500-bp product). A plasmid containing the wt *BGS13* gene and reverse transcription reaction mixtures lacking transcriptase were used as the templates for positive- and negative-control reactions, respectively. The PCR products were then analyzed by agarose gel electrophoresis.

Cloning of hybrid *Remi-bgs13* cDNA. The hybrid *Remi-bgs13* mRNA was reverse transcribed, amplified, and cloned using the SMARTer RACE 5'/3' kit (Clontech Laboratories, Mountain View, CA) according to the manufacturer's instructions, with the following specifications. Briefly, total RNA was isolated from *bgs13* strain cells grown overnight in YPD medium by a standard procedure adapted for total yeast RNA isolation (46). Approximately 2 µg of total RNA was used in the cDNA synthesis reaction, after which 90 µl of Tris-EDTA (TE) buffer was added to dilute the first-strand cDNA synthesis reaction mixture. The initial 5'-RACE reaction mixture contained 2 µl of a 5 mM solution of the *Bgs13*antisense1201 primer (GATTACGCCAAGCTTGTAAAGC AGAATCTGCCCGCAGGTGCTA), using 25 cycles of the program 94°C for 30 s, 68°C for 30 s, and 72°C for 3 min. After gel electrophoresis indicated a 1,000- to 1,300-bp product from this first 5'-RACE reaction, a nested PCR (optional, according to the kit directions) containing 5 µl of a 1:50 dilution of this reaction mixture, 25 µl of 2×SeqAmp buffer (from the kit), 1 µl of SeqAmp DNA polymerase (from the kit), 17 µl of distilled water, 1 µl of 10 µM *Bgs13*antisense1001 primer (GATTACGCCAAGCTTGC GGCTGTCTGCTCTCCCTGCC), and 1 µl of 10 µM universal primer short (from the kit) was performed using the program described above. The PCR products were gel purified using the NucleoSpin gel and PCR clean-up kit (included with the SMARTer RACE 5'/3' kit), according to the manufacturer's instructions. These purified fragments were ligated into linearized pRACE vectors using the In-Fusion HD cloning kit and were transformed by heat shock into Stellar competent *E. coli* cells (included with the SMARTer RACE 5'/3' kit), according to the manufacturer's instructions. Transformants were plated on LB agar plates supplemented with ampicillin. After colonies were grown overnight in 3 ml of LB containing antibiotic, their plasmids were isolated, and the inserts were characterized by restriction enzyme digestion followed by sequencing.

***BGS13* knockout strain construction.** The plasmid used to perform a conventional knockout of *BGS13*, named pKdSC2, was constructed as follows. First, the *S. cerevisiae HIS4* gene (47) was inserted into pBluescript SK II to create pMS4. Then, a fragment containing approximately 500 bp of 3' *BGS13* genomic sequence was generated with PCR using the primers 5' LL1BACKBamHI (TTGGATCCCATACTGGGCAAT TGTGTGC) and 3' LL1BACKSacI (TTGAGCTCGGTTCTCGTAAGAATGGA). The PCR product was digested with BamHI and SacI and inserted into the same sites of pMS4 to construct pKdSC1. A fragment containing the first approximately 500 bp of 5' *BGS13* coding sequence was then amplified by using the primers 5' LL1FRONTKpnI (GAGGTACCTGTGACACCAAGCAATGATGA) and 3' LL1FRONTPstI (GACTGC AGCGTGGTAATTCTTCAAAGCCA). The PCR product was digested with KpnI and PstI and inserted into the same sites of pKdSC1 to construct pKdSC2. pKdSC2 contains *S. cerevisiae HIS4* flanked by 5' and 3' *BGS13* sequences to promote homologous recombination. The knockout sequence was liberated by digestion with KpnI and SacI, gel purified, and then transformed into yGS115 (*his4*). His⁺ transformants were selected on YND medium (both with and without 1 M sorbitol) and subjected to colony PCR using a forward primer located in the *BGS13* promoter region and a reverse primer located within *P. pastoris HIS4*. A chromosomal *BGS13* knockout would be expected to produce a 1.2-kb PCR product.

The creation of *BGS13* knockout strains was also attempted using a CRISPR/Cas9 system developed for *P. pastoris* (22). Briefly, six plasmids (kind gifts from Anton Glieder, Technical University of Graz) were utilized, one containing gRNA sequences of *BGS13* coding sequence positions 1069 to 1088 (pKO13_gRNA1), a second containing coding sequence positions 1049 to 1068 (pKO13_gRNA2), and a third containing coding sequence positions 816 to 836 (pKO13_gRNA3) (position 1 represents the A of the initiation codon ATG) in sets of vectors with either Zeocin or G418 resistance genes. As a control, a plasmid harboring no *BGS13* gRNA sequence was also utilized (pKO13_gRNA0). The undigested plasmids were transformed into competent yJC100 or ku70 cells (19), and the cells were selected for antibiotic resistance. All groups of transformants were purified by single-streak isolation and were subjected to colony PCR using the primers *BGS13*656-680for (CCAAGAAATTAGAAACGTTGGTTTC) and *BGS13*1189-1165rev (GCTGACGAATAGCTCCATGACGACC), which amplified approximately 530 nucleotides of the chromosomal *BGS13* coding sequence, containing all three of the CRISPR/Cas9 target sites. The PCR products were purified and sequenced to confirm the predicted mutations. Alignments between CRISPR transformant and wt *BGS13* DNA were performed with SnapGene (GSL Biotech, Chicago, IL).

Plasmid constructions. The *Bgs13p* overexpression construct, pKdSC5, was produced by amplifying the entire *BGS13* coding sequence without the stop codon with the primers 5'LL1CDSXhoI (GCCTCGA GATGTGACAGACAAGC) and 3'LL1CDSNotI (AAGCGGCCGAGTGTGATCATCG). The resultant PCR product was inserted into the pPICZαB vector with the restriction enzymes XhoI and NotI. The pKdSC5 vector has a Zeocin-selectable resistance marker and *BGS13* coding sequence, fused in frame with C-terminal *c-myc* and His₆ tags, under the control of the *AOX1* promoter.

pAH1 was constructed to express the *Remi-bgs13* hybrid transcript under the control of the *AOX1* promoter. It contained 12 codons (initiated by an ATG) originating from the pREMI plasmid fused in frame to codon 148 to the stop codon of the *BGS13* coding sequence, with C-terminal *c-myc* and His₆ tags. It was constructed by amplifying the complete *Remi-bgs13* coding sequence from the chromosomal DNA of the *bgs13* strain using colony PCR (7) with the primers AH5'XhoIhulk (GGCTCGAGATGAGATCA GATCGTAAAACG) and 3' LL1CDSNotI (AAGCGGCCGAGTGTGATCATCG). The 3-kb PCR product was digested with restriction enzymes XhoI and NotI and inserted into the corresponding sites of pPICZB to create pAH1.

pBGS13-EGFP, which contains the wt *Bgs13* coding sequence fused to a C-terminal EGFP under the control of the *AOX1* promoter, was constructed by combining the 6-kb NotI-BamHI fragment of pKdSC5 with the 1.4-kb NotI-BamHI fragment pJGBG-EGFP (7). pREMI-BGS13-EGFP was constructed by digesting pBGS13-EGFP with HindIII and SphI and replacing the 2-kb fragment containing a portion of the *BGS13* coding sequence with a 1.9-kb HindIII-SphI fragment from pAH1 containing the corresponding portion of the *Remi-bgs13* coding sequence. Thus, pREMI-BGS13-EGFP expresses the *Remi-bgs13* hybrid fused to a C-terminal EGFP under the control of the *AOX1* promoter.

pAMI, which contains the *AOX1* promoter driving the expression of the MAT α -SLPI-c-myc-His₆ fusion, causes SLPI-c-myc-His₆ to be secreted into the ECM; its construction was described previously (23). pKanJV4, which contains the *AOX1* promoter driving the expression of the MAT α -MBP-EGFP fusion in a pKanaB vector, was described previously (12).

***P. pastoris* transformation.** Transformations of *P. pastoris* were performed by the electrotransformation method, as described (48). Plasmids were linearized at unique sites in the *AOX1* promoter with restriction enzymes SacI or MssI, purified with the DNA Clean and Concentrator kit (Zymo Research), and electroporated into competent yJC100 cells, yDT39 cells, or *bgs13* strain cells. Transformed cells were allowed to recover for 1 h at 30°C in 1 ml of a 50% 1 M sorbitol/50% YPD solution and then were plated on selective medium. For selection of *P. pastoris* transformants, Zeocin was added to a final concentration of 100 μ g/ml and G418 was added to a final concentration of 500 μ g/ml (49). Transformed colonies were then purified by streaking for isolated colonies on selective medium.

Small-scale induction. Cells were grown in a sterile 96-deep-well-plate (DWP) format for enzymatic assays (50, 51). Five hundred microliters of sterile water was added to the perimeter of the plate to prevent evaporation. Next, 250 μ l of liquid buffered minimal medium with dextrose (BMD), along with any amino acid supplements needed, was added to the wells that were designated to hold the cell cultures. Isolated colonies were selected from fresh plates and inoculated into their designated wells containing 1 \times BMD. Parafilm was wrapped around the edges of the DWP and the corners were taped to block evaporation. The DWP was placed in a 28°C shaking incubator at 325 rpm. After 48 h, 5- μ l aliquots of cell culture from randomly selected wells were added to glucose test strips to confirm that all of the glucose had been exhausted. Subsequently, the cells were induced with 250 μ l of 2 \times BMMY, yielding a final methanol concentration of 0.5%. The plate was sealed with Parafilm and placed back in the shaking incubator with the same settings. During the next two consecutive 24-h periods, 50 μ l of 10 \times buffered minimal medium with methanol (BMM) was added to each well. On the sixth day, after a total of 72 h of methanol induction, the OD₆₀₀ of each sample was measured at a 1:20 dilution. The samples were transferred from the wells into 1.5-ml microcentrifuge tubes, centrifuged at maximum speed for 1 min, and either stored in the -80°C freezer or used immediately for enzymatic assays.

Large-scale expression. Cultures were first grown overnight in YPD medium to stationary phase. On the second day, the OD₆₀₀ was measured, and 5.0 OD₆₀₀ units of each culture were pelleted for 5 min at 2,000 \times g at room temperature. The cells were suspended in 5 ml of BMGY in a 50-ml conical centrifuge tube. On the third day, the OD₆₀₀ was measured, and 10 OD₆₀₀ units of each culture were pelleted for 5 min at 2,000 \times g at room temperature. The cells were suspended in 10 ml of BMMY in a 50-ml conical centrifuge tube. The cultures were induced for 48 and 72 h at 28°C with shaking (225 rpm), with the addition of methanol to 0.5% (vol/vol) every 24 h to compensate for losses resulting from evaporation and metabolism. At each time point, the OD₆₀₀ of each culture was measured, and 1.0 ml was centrifuged at 10,000 \times g for 1 min to separate cells from extracellular supernatant. The supernatants were transferred to new microcentrifuge tubes, and Protease Arrest protease inhibitor (G Biosciences, St. Louis, MO) was added. Pellets and supernatants were immediately frozen and stored at -80°C. This protocol was also scaled up 10-fold (100 ml of BMMY) for larger preparations of MBP fusion peptides.

PKC assays. *P. pastoris* strains were grown overnight in BMMY to approximately 10 OD₆₀₀ and were harvested by centrifugation at 13,000 \times g for 1 min. After the ECM was removed, 500 μ l of chilled phosphate-buffered saline (PBS) and 1 μ l of 1 M phenylmethylsulfonyl fluoride (PMSF) were added to each pellet. After 150 μ l of chilled glass beads (500- to 600- μ m) was added to each sample, the lips of the tubes were cleaned with cotton swabs so that the tubes could seal well. The tubes were closed and vortex-mixed for a total of 3 min, consisting of three cycles of 1 min of vortex-mixing followed by 1 min on ice. The tubes were then centrifuged at 13,000 \times g for 5 min at 4°C. The supernatant was transferred to a fresh tube and kept on ice. PKC activity was measured using a PKC activity kit (Enzo Life Sciences, Farmingdale, NY), according to the manufacturer's directions.

Spot Western blotting. Spot Western blots were used to detect the presence of antigen in the ECM or intracellular extracts of recombinant *P. pastoris* cells (50). The vacuum attached to the 96-well Spot Blot apparatus (Topac, Boston, MA) was turned on, and the amount of supernatant that was added to the wells on the prewet nitrocellulose membrane was measured, to equal the OD₆₀₀ of the sample with the lowest OD₆₀₀ measurement. The spotted nitrocellulose membrane was allowed to dry in a 60°C oven for 5 min. The membrane was then soaked in 1 \times PBS while the SNAP ID protein detection system blot holder (Millipore, Billerica, MA) was wet with water. The nitrocellulose membrane was inserted into the blot holder, followed by a spacer sheet. The closed blot holder was placed in the SNAP ID apparatus, attached to a vacuum. With the vacuum turned on, 30 ml of I-Block (Thermo Fisher Scientific) solution (1 \times PBS with 0.2% I-Block and 0.1% Tween 20) was added to the membrane. The vacuum was turned off before incubation of the membrane with 3 ml of I-Block solution containing 10 μ l of the primary antibody, i.e., mouse anti-GFP, rabbit anti-MBP, or mouse anti-c-myc (Santa Cruz Biotechnology, Santa Cruz, CA). After 10 min of incubation with the primary antibody, the vacuum was turned on again, and the membrane was washed three times with a total of 100 ml of wash buffer (1 \times PBS with 0.1% Tween 20). The membrane was then incubated for 10 min in 3 ml of I-Block containing a goat anti-mouse IgG

or goat anti-rabbit IgG secondary antibody, conjugated to alkaline phosphatase (Applied Biosystems, Foster City, CA), with the vacuum off. The membrane was then washed three times with wash buffer, as described previously, before it was incubated for 5 min in a petri dish containing 20 ml of femtoLUCENT PLUS-AP 1 × Tris-buffered saline with Tween (G Biosciences). The blot was laid flat on a plastic-wrap surface, and 2 ml of the femtoLUCENT PLUS-AP detection reagent was added dropwise onto the membrane. After 5 min of incubation at room temperature, the detection reagent was drained off. The membrane was placed in a plastic envelope or wrap and developed using the Bio-Rad ChemiDoc XRS+ imaging system (Bio-Rad, Hercules, CA), with exposure times of 1 to 2 min. Signals were quantified with Bio-Rad Image Lab software.

Polyacrylamide gel electrophoresis and Western blot analysis. Protein concentrations were determined using the Pierce (Rockford, IL) bicinchoninic acid (BCA) protein assay kit with BSA as the standard. Either equivalent amounts of protein or volumes of ECM from equivalent numbers of cells were electrophoresed on SDS-PAGE gels. The proteins were either stained for total protein visualization using GelCode Blue (Pierce, Rockford, IL) or Silver Snap II (Pierce) stain or analyzed by Western blotting. For immunoblotting, proteins were transferred onto nitrocellulose membranes using an iBlot apparatus (Life Technologies), according to the manufacturer's instructions. Immunoblots were processed as described above, using the SNAP i.d. system and femtoLUCENT reagents. The anti-PDI antibody was a generous gift from Carl Batt (Cornell University, Ithaca, NY).

Transmission electron microscopy. Transmission electron microscopy was performed as described previously (52).

Fluorescence microscopy. (i) Growth and induction. Fresh colonies were inoculated into 5 ml of BMY in 50 ml conical tubes. These cultures were incubated overnight at 28°C, at 325 rpm. Next, 2 OD₆₀₀ units of the cells were centrifuged and resuspended in 2 ml of BMMY, in new 50-ml conical tubes, to start the induction with a concentration of 1 OD₆₀₀ unit/ml. The cell cultures were incubated again in a 28°C shaking incubator for 5 to 6 h.

(ii) Vacuolar staining with the FM 4-64 dye. Some strains were stained with the FM 4-64 dye (Life Technologies). This dye stains the vacuolar membranes in *P. pastoris*, which serves as a point of reference for visualizing the localization of fluorescent proteins inside the cells (53, 54). When the cells were switched to BMMY, 2 μl of FM 4-64 (1 mg/ml) was added to the BMMY-cell mixture. Cell cultures were incubated for 5 to 6 h in a 28°C shaking incubator before the cells were visualized with fluorescence microscopy.

(iii) Visualization with fluorescence microscopy. After induction for 5 to 6 h, the cells were centrifuged in 50-ml conical tubes at 3,000 × *g* for 5 min and resuspended in 2 ml of fresh 1 M sorbitol or sterile water. The samples were centrifuged briefly for pelleting. The sorbitol or water was discarded and 500 μl of fresh 1 M sorbitol or water was added to resuspend the cells. Then, 5 μl of each sample was added to dried 1% agarose in water on microscope slides (Fisher Scientific, Pittsburgh, PA), and a coverslip (Corning Life Sciences, Lowell, MA) was placed over each sample. Confocal fluorescence images were acquired with a Leica DMIRE2 inverted fluorescence microscope using MetaMorph software (Molecular Devices) and a Yokogawa CSU-X1 spinning disc confocal system with a QuantEM:5125C camera. Excitation and emission wavelengths were as follows: excitation at 491 nm and emission at 525 ± 25 nm for visualization of EGFP and excitation at 561 nm and emission at 605 ± 25.5 nm for visualization of FM 4-64 dye.

CWI assays. CWI assays were performed using both Cr and Cfw, as described previously (24). Briefly, YPD plates were made with different concentrations of Cr (0, 10, 20, and 40 μg/ml) and Cfw (0, 1, 2, and 5 μg/ml). Serial dilutions (1, 10⁻¹, 10⁻², 10⁻³, and 10⁻⁴) of 1 OD₆₀₀ unit were of the *bgs13* strain and its parent strain yDT39, as well as FWK1 and its parent strain KU70. FWK1 is a Δ*och1* mutant that served as a positive control. Five microliters of each dilution was spotted onto all plates, which were incubated at 30°C for 3 days, and cells were analyzed for viability.

Cell wall porosity assay. The permeability of the wt strain (yDT39-pAM1) and *bgs13* strain (ybgs13-pAM1) cell walls was measured using a protocol adapted for several different fungal species (55). In addition, the assay was performed with a mutant strain (FWK1) with a known cell wall defect in the *OCH1* gene and its parent strain (Ku70), for comparison (30). Briefly, overnight cultures of cells grown in YPD medium were diluted in fresh medium to an OD₆₀₀ of 0.1 at 28°C and then were allowed to grow to an OD₆₀₀ of approximately 1. For each strain, approximately 8 OD₆₀₀ units of cells were centrifuged at 3,500 × *g* for 7 min at room temperature. The supernatant was discarded, and the cell pellet was washed three times with 0.22-μm sterile-filtered Milli-Q water. The cells were then resuspended in 10 mM Tris (pH 7.4) to a final OD₆₀₀ of approximately 2.0, and the resuspension was divided into three 1.5-ml centrifuge tubes with an approximate volume of 0.9 ml in each. To each 0.9 ml of cell suspension was added either (i) 100 μl of 10× poly-L-lysine (30 to 70 kDa; Sigma-Aldrich, St. Louis, MO) (100 μg/ml in 10 mM Tris [pH 7.4]), (ii) 100 μl of 10× DEAE-dextran (500 kDa; Sigma-Aldrich) (50 μg/ml in 10 mM Tris [pH 7.4]), or (iii) 100 μl of 10 mM Tris (pH 7.4). The cell suspensions were then incubated at 28°C for 30 min in shaking incubator, at 200 rpm. The cells were centrifuged two times for 2 min at 10,000 × *g* to isolate the supernatant. The A₂₆₀ reading for each supernatant was taken to measure the UV-absorbing compounds, using the supernatant from cells incubated in only 10 mM Tris buffer (pH 7.4) as a blank. The assay was performed on bioreplicate samples in duplicate. The relative cell wall porosity was defined as follows: porosity (%) = [(A₂₆₀ of DEAE-dextran)/(A₂₆₀ of poly-L-lysine)] × 100%.

Mass spectrometry and proteomic analysis of proteins found in the ECM. yDT39-pKanJV4 (wt) and ybgs13-pKanJV4 cultures were grown overnight in YPD medium to stationary phase. OD₆₀₀ measurements were obtained, and 5.0 OD₆₀₀ units of each culture were pelleted and resuspended in 10 ml of BMD with histidine and methionine. Cultures were grown for 24 h, and then 50 OD₆₀₀ units of wt strain

culture and 100 OD₆₀₀ units of *bgs13* strain culture (to compensate for the lower growth rate) were pelleted and resuspended in 50 ml of BMM with histidine and methionine. Cultures were induced for 48 h at 28°C, with shaking at 225 rpm; methanol was added to 0.5% at 24 h postinduction, to compensate for losses resulting from evaporation and metabolism. At harvest, the OD₆₀₀ of each culture was measured, cells were centrifuged, and the supernatant was filtered (0.22 μm) to remove remaining cell particulates. Cell pellets and supernatants were immediately frozen and stored at -80°C.

Supernatant total protein concentrations were measured at 280 nm for both strains, using a Nano-Drop spectrophotometer (Thermo Fisher Scientific). Triplicate aliquots containing 2 mg of protein were prepared, and each replicate was spiked (1 part spiked reference proteins/500 parts proteins) with protein standards, including BSA (Thermo Fisher Scientific) and horse myoglobin (Sigma-Aldrich), for subsequent label-free proteomics quantitation analyses. Aliquots were precipitated using acetone (-20°C for 3 h). Proteins were dried, pelleted, and then resuspend in 200 μl of 3 M urea-100 mM Tris (pH 7.8). Precipitated protein concentrations were determined using the same methods as above, and then all samples were diluted to standardize concentrations (0.5 μg/μl; 50 μg total protein) prior to sample preparation for proteomics. Proteins were reduced with 5 mM DTT (Gold Biotechnology, St. Louis, MO) for 30 min at room temperature and were alkylated with 15 mM iodoacetamide [IAA] (Sigma-Aldrich) for 30 min at room temperature in the dark. Unreacted IAA was quenched by addition of 20 μl of 200 mM DTT and incubation for an additional 30 min. Each reaction was diluted with 3 volumes of sterile water (~750 μl), to reduce the urea concentration to <2 M, and then digested overnight at 37°C using trypsin (Promega, San Louis Obispo, CA) (1 part trypsin/10 parts proteins). Digestions were halted with the addition of trifluoroacetic acid (TFA) to a final volume of 5% and digested peptides were purified using OMIX C₁₈ spin columns, according to the manufacturer's instructions (Agilent Technologies, Santa Clara, CA). Samples were then diluted, lyophilized, and resuspended in 40 μl of 0.1% formic acid in high-performance liquid chromatography (HPLC)-grade water; peptide samples were diluted to 150 ng/μl. All samples were stored at -80°C until mass spectrometry analysis.

HPLC-MS/MS. For each sample, 5 μl was loop injected by a Dionex Ultimate 3000 autosampler onto an EASY-Spray C₁₈ liquid chromatography column (75 μm i.d. by 15 cm, 100 Å; Thermo Fisher Scientific) held at 35°C for HPLC. Flow rates were kept at 300 nl/min, set to 140 min. Solvents A and B were 0.1% formic acid in water and 0.1% formic acid in acetonitrile, respectively. Solvent B was used as follows: 3% for 5 min, 3% to 28% in 75 min, 28% to 45% in 25 min, 45% to 95% in 5 min, 95% for 5 min, return to 3% in 5 min, and 2% for 25 min.

Mass spectrometry analysis was performed using an Orbitrap Fusion Tribrid mass spectrometer equipped with nanospray HPLC (Thermo Fisher Scientific), operated in a data-dependent acquisition (DDA) manner via Xcalibur 4.0 software (Thermo Fisher Scientific). Briefly MS1 spectra were collected by using the Orbitrap mass analyzer; precursor ions were selected via DDA using a quadrupole mass filter and then were fragmented using higher energy collisional dissociation in the collision cell. Instrument and data acquisition settings were the same as reported previously (56), with the exception of the scan range (200 to 1,400 Da), MS1 Orbitrap resolution (120,000), scan time (10 to 130 min), MS/MS Orbitrap resolution (30,000), and MS/MS maximum injection time (150 ms).

Protein identification. Analysis of MS/MS data was performed via Proteome Discoverer 2.2.0.388 (Thermo Fisher Scientific). Peptide spectra were searched in the complete UniProt/Swiss-Prot database (downloaded on 13 February 2018) using SEQUEST. To identify any associated contaminants that might have arisen during sample preparation, spectra were searched in the common Repository of Adventitious Proteins (cRAP) (<https://www.thegpm.org/crap/index.html>). Search parameters were the same as reported previously (56). False-discovery rates for peptide spectral matches and peptides were estimated by searching reversed decoy databases generated from the UniProt/Swiss-Prot and cRAP databases. Results were filtered to remove identified contaminants. Peptides with target false-discovery rates of <1% were retained. For proteins to be categorized as unique, ≥2 unique peptides that mapped back to the spectra were required.

Protein quantitation. Protein quantitation was performed using Proteome Discoverer 2.2.0.388 (Thermo Fisher Scientific). To align chromatographic runs for each biological condition, the feature mapper node was used with a maximum retention time shift of 10 min, a mass tolerance of 10 ppm, and a minimum signal/noise threshold of 5 for feature linking mapping. MS/MS data were filtered to retain only proteins that had ≥2 unique peptide hits and were identified in all samples with high levels of confidence. Biological replicates were grouped by condition. Quantitative abundances were calculated, normalized to those of reference proteins (BSA and horse myoglobin), and scaled with a label-free method using the precursor ion quantifier node in Proteome Discoverer 2.2. Abundance ratio calculations were made by using summed abundance values. An analysis of variance for individual proteins was performed to determine whether protein abundances differed significantly ($P \leq 0.05$) between samples. Abundance ratio and log₂(fold change) values were calculated for the sample comparisons between wt and mutant strains.

DTT extraction of cell wall proteins. DTT extracts of wt strain (yDT39-pKanJV4) and *bgs13* strain (ybgs13-pKanJV4) cells were prepared according to a described previously protocol (27). pKanJV4 expresses an MBP-EGFP fusion protein under the control of the AOX1 promoter. Briefly, 40 OD₆₀₀ units of cells were grown to early stationary phase (OD₆₀₀ of ~10) overnight in either BMM or BMMY, harvested by centrifugation (5 min at 300 × g), washed twice with 10 ml of water, and resuspended (0.5 OD₆₀₀ unit equivalents/μl) in extraction buffer (50 mM Tris [pH 7.5], 5 mM DTT). As negative controls, both strains were resuspended in 50 mM Tris (pH 7.5) alone. The cell suspensions were shaken in a multivortex apparatus for 2 h at 4°C, and the supernatants were used for further analysis. An aliquot of the supernatant was removed, mixed with 2× Laemmli sample buffer, boiled for 5 min at 100°C, and

fractionated by SDS-PAGE (Bio-Rad Mini-Protean TGX 4 to 20% gradient gels). Fractionated proteins were visualized by silver staining according to the manufacturer's protocol (Pierce silver stain kit; Thermo Fisher Scientific).

Mass spectrometry and proteomics of proteins extracted from the cell wall. From the DTT extraction of cell wall proteins, supernatant total protein concentrations for both strains were measured at 280 nm using a Nanodrop spectrophotometer (Thermo Fisher Scientific). Duplicate aliquots containing 120 μg of protein were prepared. Aliquots were precipitated using acetone (at -20°C for 3 h). Proteins were dried, pelleted, and then resuspended in 200 μl of 3 M urea-100 mM Tris (pH 7.8). Precipitated protein concentrations were determined using the same methods as described above, and then all samples were diluted to standardized concentrations (approximately 0.21 $\mu\text{g}/\mu\text{l}$; 25 μg total protein) prior to proteomics sample preparation. Prior to sample preparation for tryptic digestion, each replicate was spiked (1 part spiked reference proteins/500 parts proteins) with protein standards, including BSA and horse myoglobin, for subsequent label-free proteomics quantitation analyses. Samples were reduced in 5 mM DTT (Gold Biotechnology) for 30 min at room temperature and alkylated using 15 mM IAA (Sigma-Aldrich) for 30 min in the dark at room temperature. Unreacted IAA was quenched by addition of 20 μl of 200 mM DTT and incubation for an additional 30 min. Each reaction mixture was then diluted with 3 volumes of sterile water (~ 750 μl), to reduce the urea concentration to <2 M, and digested overnight at 37°C using trypsin (Promega) (1:10 trypsin/protein). The digestion was halted with the addition of TFA, and digested peptides were purified using OMIX C_{18} spin columns, according to the manufacturer's instructions (Agilent Technologies). Samples were then diluted and lyophilized. Lyophilized samples were resuspended in 40 μl of 0.1% formic acid in HPLC-grade water; peptide samples were diluted to 150 ng/ μl . All samples were stored at -80°C until mass spectrometry analysis. Subsequent HPLC-MS/MS, protein identification, and protein quantitation procedures and parameters were the same as those used for the ECM.

Cytoplasmic and membrane-associated protein extraction. Protein extractions from soluble cytoplasmic and insoluble membrane-associated fractions were performed according to a previous extraction procedure (6). Cells (OD_{600} of 4) stored at -80°C were thawed, washed in PBS (pH 7.4), and then resuspended in yeast lysis buffer (50 mM sodium phosphate [pH 7.4], 1 mM PMSF, 1 mM EDTA, 5% [vol/vol] glycerol). An equal amount of acid-washed glass beads was added, and cells were lysed by vortex-mixing at maximum speed 10 times for 1 min, with 1-min periods on ice. The lysate was centrifuged at $10,000 \times g$ for 30 min at 4°C . The supernatant, containing mainly cytoplasmic proteins, was collected and designated the soluble fraction. The remaining pellet with cell debris and glass beads was resuspended in 100 μl of lysis buffer containing 2% (wt/vol) SDS and was centrifuged at $4,000 \times g$ for 5 min at 4°C . The supernatant was collected as designated the membrane-associated fraction. Extraction and detection of PDI was also performed on yJC100-pAM1-pPICZPDI cells, as a positive control (23).

SUPPLEMENTAL MATERIAL

Supplemental material for this article may be found at <https://doi.org/10.1128/AEM.01615-19>.

SUPPLEMENTAL FILE 1, PDF file, 1.2 MB.

ACKNOWLEDGMENTS

This work was supported by NIH AREA grants GM65882-03 and GM129758-01, as well as Scholarly and Artistic Activity grants from University of the Pacific to J.L.-C. and G.P.L.-C. This research was also funded by a National Science Foundation grant (grant DBI 1531417) to C.A.V.

REFERENCES

1. Yang Z, Zhang Z. 2018. Engineering strategies for enhanced production of protein and bio-products in *Pichia pastoris*: a review. *Biotechnol Adv* 36:182–195. <https://doi.org/10.1016/j.biotechadv.2017.11.002>.
2. Purkarthofer T, Dib I, Trummer-Godl E. 2017. What about Pichia? *Eur Biopharm Rev* 2017(summer):22–25.
3. Cereghino JL, Cregg JM. 2000. Heterologous protein expression in the methylotrophic yeast *Pichia pastoris*. *FEMS Microbiol Rev* 24:45–66. <https://doi.org/10.1111/j.1574-6976.2000.tb00532.x>.
4. Juturu V, Wu JC. 2018. Heterologous protein expression in *Pichia pastoris*: latest research progress and applications. *ChemBiochem* 19: 7–21. <https://doi.org/10.1002/cbic.201700460>.
5. Idiris A, Tohda H, Kumagai H, Takegawa K. 2010. Engineering of protein secretion in yeast: strategies and impact on protein production. *Appl Microbiol Biotechnol* 86:403–417. <https://doi.org/10.1007/s00253-010-2447-0>.
6. Damasceno LM, Anderson KA, Ritter G, Cregg JM, Old LJ, Batt CA. 2007. Cooverexpression of chaperones for enhanced secretion of a single-chain antibody fragment in *Pichia pastoris*. *Appl Microbiol Biotechnol* 74:381–389. <https://doi.org/10.1007/s00253-006-0652-7>.
7. Larsen S, Weaver J, de Sa Campos K, Bulahan R, Nguyen J, Grove H, Huang A, Low L, Tran N, Gomez S, Yau J, Ilustrisimo T, Kawilarang J, Lau J, Tranphung M, Chen I, Tran C, Fox M, Lin-Cereghino J, Lin-Cereghino GP. 2013. Mutant strains of *Pichia pastoris* with enhanced secretion of recombinant proteins. *Biotechnol Lett* 35:1925. <https://doi.org/10.1007/s10529-013-1290-7>.
8. Stadlmayr G, Benakovitsch K, Gasser B, Mattanovich D, Sauer M. 2010. Genome-scale analysis of library sorting (GALibSo): isolation of secretion enhancing factors for recombinant protein production in *Pichia pastoris*. *Biotechnol Bioeng* 105:543–555. <https://doi.org/10.1002/bit.22573>.
9. Levin DE. 2005. Cell wall integrity signaling in *Saccharomyces cerevisiae*. *Microbiol Mol Biol Rev* 69:262–291. <https://doi.org/10.1128/MMBR.69.2.262-291.2005>.
10. Levin DE. 2011. Regulation of cell wall biogenesis in *Saccharomyces cerevisiae*: the cell wall integrity signaling pathway. *Genetics* 189: 1145–1175. <https://doi.org/10.1534/genetics.111.128264>.
11. Garcia R, Sanz AB, Rodriguez-Pena JM, Nombela C, Arroyo J. 2016. Rlm1 mediates positive autoregulatory transcriptional feedback that is essen-

- tial for SlT2-dependent gene expression. *J Cell Sci* 129:1649–1660. <https://doi.org/10.1242/jcs.180190>.
12. Moua PS, Gonzalez A, Oshiro KT, Tam V, Li ZH, Chang J, Leung W, Yon A, Thor D, Venkatram S, Franz AH, Risser DD, Lin-Cereghino J, Lin-Cereghino GP. 2016. Differential secretion pathways of proteins fused to the *Escherichia coli* maltose binding protein (MBP) in *Pichia pastoris*. *Protein Expr Purif* 124:1–9. <https://doi.org/10.1016/j.pep.2016.04.005>.
 13. Fitzgerald I, Glick BS. 2014. Secretion of a foreign protein from budding yeasts is enhanced by cotranslational translocation and by suppression of vacuolar targeting. *Microb Cell Fact* 13:125. <https://doi.org/10.1186/s12934-014-0125-0>.
 14. Marsalek L, Gruber C, Altmann F, Aleschko M, Mattanovich D, Gasser B, Puxbaum V. 2017. Disruption of genes involved in CORVET complex leads to enhanced secretion of heterologous carboxylesterase only in protease deficient *Pichia pastoris*. *Biotechnol J* 12:1600584. <https://doi.org/10.1002/biot.201600584>.
 15. Denis V, Cyert MS. 2005. Molecular analysis reveals localization of *Saccharomyces cerevisiae* protein kinase C to sites of polarized growth and Pkc1p targeting to the nucleus and mitotic spindle. *Eukaryot Cell* 4:36–45. <https://doi.org/10.1128/EC.4.1.36-45.2005>.
 16. Schroder LA, Glick BS, Dunn WA. 2007. Identification of pexophagy genes by restriction enzyme-mediated integration. *Methods Mol Biol* 389:203–218. https://doi.org/10.1007/978-1-59745-456-8_15.
 17. Leeds P, Peltz SW, Jacobson A, Culbertson MR. 1991. The product of the yeast UPF1 gene is required for rapid turnover of mRNAs containing a premature translational termination codon. *Genes Dev* 5:2303–2314. <https://doi.org/10.1101/gad.5.12a.2303>.
 18. Schmitz HP, Lorberg A, Heinisch JJ. 2002. Regulation of yeast protein kinase C activity by interaction with the small GTPase Rho1p through its amino-terminal HR1 domain. *Mol Microbiol* 44:829–840. <https://doi.org/10.1046/j.1365-2958.2002.02925.x>.
 19. Naatsaari L, Mistlberger B, Ruth C, Hajek T, Hartner FS, Glieder A. 2012. Deletion of the *Pichia pastoris* KU70 homolog facilitates platform strain generation for gene expression and synthetic biology. *PLoS One* 7:e39720. <https://doi.org/10.1371/journal.pone.0039720>.
 20. Higgins DR, Cregg JM. 1998. Introduction to *Pichia pastoris*, p 1–15. In Higgins DR, Cregg JM (ed), *Pichia protocols*. Humana Press, Totowa, NJ.
 21. Schwarzhans JP, Wibberg D, Winkler A, Luttermann T, Kalinowski J, Friehs K. 2016. Integration event induced changes in recombinant protein productivity in *Pichia pastoris* discovered by whole genome sequencing and derived vector optimization. *Microb Cell Fact* 15:84. <https://doi.org/10.1186/s12934-016-0486-7>.
 22. Weninger A, Hatzl AM, Schmid C, Vogl T, Glieder A. 2016. Combinatorial optimization of CRISPR/Cas9 expression enables precision genome engineering in the methylotrophic yeast *Pichia pastoris*. *J Biotechnol* 235: 139–149. <https://doi.org/10.1016/j.jbiotec.2016.03.027>.
 23. Li Z, Moy A, Gomez SR, Franz AH, Lin-Cereghino J, Lin-Cereghino GP. 2010. An improved method for enhanced production and biological activity of human secretory leukocyte protease inhibitor (SLPI) in *Pichia pastoris*. *Biochem Biophys Res Commun* 402:519–524. <https://doi.org/10.1016/j.bbrc.2010.10.067>.
 24. Ram AF, Klis FM. 2006. Identification of fungal cell wall mutants using susceptibility assays based on Calcofluor white and Congo red. *Nat Protoc* 1:2253–2256. <https://doi.org/10.1038/nprot.2006.397>.
 25. Tang H, Wang S, Wang J, Song M, Xu M, Zhang M, Shen Y, Hou J, Bao X. 2016. N-Hypermannose glycosylation disruption enhances recombinant protein production by regulating secretory pathway and cell wall integrity in *Saccharomyces cerevisiae*. *Sci Rep* 6:25654. <https://doi.org/10.1038/srep25654>.
 26. Lesage G, Bussey H. 2006. Cell wall assembly in *Saccharomyces cerevisiae*. *Microbiol Mol Biol Rev* 70:317–343. <https://doi.org/10.1128/MMBR.00038-05>.
 27. Scrimale T, Didone L, de Mesy Bentley KL, Krysan DJ. 2009. The unfolded protein response is induced by the cell wall integrity mitogen-activated protein kinase signaling cascade and is required for cell wall integrity in *Saccharomyces cerevisiae*. *Mol Biol Cell* 20:164–175. <https://doi.org/10.1091/mbc.e08-08-0809>.
 28. Puxbaum V, Mattanovich D, Gasser B. 2015. Quo vadis? The challenges of recombinant protein folding and secretion in *Pichia pastoris*. *Appl Microbiol Biotechnol* 99:2925–2938. <https://doi.org/10.1007/s00253-015-6470-z>.
 29. De Nobel JG, Klis FM, Munnik T, Priem J, van den Ende H. 1990. An assay of relative cell wall porosity in *Saccharomyces cerevisiae*, *Kluyveromyces lactis* and *Schizosaccharomyces pombe*. *Yeast* 6:483–490. <https://doi.org/10.1002/yea.320060605>.
 30. Krainer FW, Gmeiner C, Neutsch L, Windwarder M, Pletzenauer R, Herwig C, Altmann F, Glieder A, Spadiut O. 2013. Knockout of an endogenous mannosyltransferase increases the homogeneity of glycoproteins produced in *Pichia pastoris*. *Sci Rep* 3:3279. <https://doi.org/10.1038/srep03279>.
 31. Huang CJ, Damasceno LM, Anderson KA, Zhang S, Old LJ, Batt CA. 2011. A proteomic analysis of the *Pichia pastoris* secretome in methanol-induced cultures. *Appl Microbiol Biotechnol* 90:235–247. <https://doi.org/10.1007/s00253-011-3118-5>.
 32. Krysan DJ. 2009. The cell wall and endoplasmic reticulum stress responses are coordinately regulated in *Saccharomyces cerevisiae*. *Commun Integr Biol* 2:233–235. <https://doi.org/10.4161/cib.2.3.8097>.
 33. Travers KJ, Patil CK, Wodicka L, Lockhart DJ, Weissman JS, Walter P. 2000. Functional and genomic analyses reveal an essential coordination between the unfolded protein response and ER-associated degradation. *Cell* 101:249–258. [https://doi.org/10.1016/s0092-8674\(00\)80835-1](https://doi.org/10.1016/s0092-8674(00)80835-1).
 34. Ron D, Walter P. 2007. Signal integration in the endoplasmic reticulum unfolded protein response. *Nat Rev Mol Cell Biol* 8:519–529. <https://doi.org/10.1038/nrm2199>.
 35. Raschmanová H, Zamora I, Borčinová M, Meier P, Weninger A, Mächler D, Glieder A, Melzoch K, Knejzlík Z, Kovar K. 2019. Single-cell approach to monitor the unfolded protein response during biotechnological processes with *Pichia pastoris*. *Front Microbiol* 10:335. <https://doi.org/10.3389/fmicb.2019.00335>.
 36. Guerfal M, Ryckaert S, Jacobs PP, Ameloot P, Van Craenenbroeck K, Derycke R, Callewaert N. 2010. The *HAC1* gene from *Pichia pastoris*: characterization and effect of its overexpression on the production of secreted, surface displayed and membrane proteins. *Microb Cell Fact* 9:49. <https://doi.org/10.1186/1475-2859-9-49>.
 37. Roth G, Vanz AL, Lünsdorf H, Nimt M, Rinas U. 2018. Fate of the UPR marker protein Kar2/Bip and autophagic processes in fed-batch cultures of secretory insulin precursor producing *Pichia pastoris*. *Microb Cell Fact* 17:123. <https://doi.org/10.1186/s12934-018-0970-3>.
 38. Yu XW, Sun WH, Wang YZ, Xu Y. 2017. Identification of novel factors enhancing recombinant protein production in multi-copy *Komagataella phaffii* based on transcriptomic analysis of overexpression effects. *Sci Rep* 7:16249. <https://doi.org/10.1038/s41598-017-16577-x>.
 39. Shimizu J, Yoda K, Yamasaki M. 1994. The hypo-osmolarity-sensitive phenotype of the *Saccharomyces cerevisiae hpo2* mutant is due to a mutation in PKC1, which regulates expression of β -glucanase. *Mol Gen Genet* 242:641–648. <https://doi.org/10.1007/bf00283417>.
 40. Hohenblum H, Gasser B, Maurer M, Borth N, Mattanovich D. 2004. Effects of gene dosage, promoters, and substrates on unfolded protein stress of recombinant *Pichia pastoris*. *Biotechnol Bioeng* 85:367–375. <https://doi.org/10.1002/bit.10904>.
 41. Dragosits M, Mattanovich D, Gasser B. 2011. Induction and measurement of UPR and osmotic stress in the yeast *Pichia pastoris*. *Methods Enzymol* 489:165–188. <https://doi.org/10.1016/B978-0-12-385116-1.00010-8>.
 42. Benitez EM, Stolz A, Wolf DH. 2011. Yos9, a control protein for misfolded glycosylated and non-glycosylated proteins in ERAD. *FEBS Lett* 585: 3015–3019. <https://doi.org/10.1016/j.febslet.2011.08.021>.
 43. Thor D, Xiong S, Orazem CC, Kwan AC, Cregg JM, Lin-Cereghino J, Lin-Cereghino GP. 2005. Cloning and characterization of the *Pichia pastoris MET2* gene as a selectable marker. *FEMS Yeast Res* 5:935–942. <https://doi.org/10.1016/j.femsyr.2005.03.009>.
 44. Lin-Cereghino GP, Leung W, Lin-Cereghino J. 2007. Expression of protein in *Pichia pastoris*, p 123–145. In Dyson M, Durocher Y (ed), *Expression systems: methods express*. Scion Publishing, Banbury, United Kingdom.
 45. Sambrook J, Fritsch EF, Maniatis T. 1989. *Molecular cloning: a laboratory manual*, 2nd ed. Cold Spring Harbor Laboratory Press, Cold Spring Harbor, NY.
 46. Cereghino GP, Atencio DP, Saghbini M, Beiner J, Scheffler IE. 1995. Glucose-dependent turnover of the mRNAs encoding succinate dehydrogenase peptides in *Saccharomyces cerevisiae*: sequence elements in the 5' untranslated region of the *ip* mRNA play a dominant role. *Mol Biol Cell* 6:1125–1143. <https://doi.org/10.1091/mbc.6.9.1125>.
 47. Lin-Cereghino GP, Godfrey L, de la Cruz BJ, Johnson S, Khuongsathiene S, Tolstorukov I, Yan M, Lin-Cereghino J, Veenhuis M, Subramani S, Cregg JM. 2006. Mxr1p, a key regulator of the methanol utilization pathway and peroxisomal genes in *Pichia pastoris*. *Mol Cell Biol* 26:883–897. <https://doi.org/10.1128/MCB.26.3.883-897.2006>.
 48. Lin-Cereghino J, Wong WW, Xiong S, Giang W, Luong LT, Vu J, Johnson

- SD, Lin-Cereghino GP. 2005. Condensed protocol for competent cell preparation and transformation of the methylotrophic yeast *Pichia pastoris*. *Biotechniques* 38:44–48. <https://doi.org/10.2144/05381BM04>.
49. Lin-Cereghino J, Hashimoto MD, Moy A, Castelo J, Orazem CC, Kuo P, Xiong S, Gandhi V, Hatae CT, Chan A, Lin-Cereghino GP. 2008. Direct selection of *Pichia pastoris* expression strains using new G418 resistance vectors. *Yeast* 25:293–299. <https://doi.org/10.1002/yea.1587>.
50. Lin-Cereghino GP, Stark CM, Kim D, Chang J, Shaheen N, Poerwanto H, Agari K, Moua P, Low LK, Tran N, Huang AD, Nattestad M, Oshiro KT, Chang JW, Chavan A, Tsai JW, Lin-Cereghino J. 2013. The effect of alpha-mating factor secretion signal mutations on recombinant protein expression in *Pichia pastoris*. *Gene* 519:311–317. <https://doi.org/10.1016/j.gene.2013.01.062>.
51. Weis R, Luiten R, Skranc W, Schwab H, Wubbolts M, Glieder A. 2004. Reliable high-throughput screening with *Pichia pastoris* by limiting yeast cell death phenomena. *FEMS Yeast Res* 5:179–189. <https://doi.org/10.1016/j.femsyr.2004.06.016>.
52. Yount BA, Lin-Cereghino J, Lin-Cereghino GP, Fox MM. 2006. Preparation of the yeast *Pichia pastoris* for transmission electron microscopy. *Microsc Today* 14:36–37. <https://doi.org/10.1017/S155192950005865X>.
53. Farre JC, Shirahama-Noda K, Zhang L, Booher K, Subramani S. 2007. Localization of proteins and organelles using fluorescence microscopy. *Methods Mol Biol* 389:239–250. https://doi.org/10.1007/978-1-59745-456-8_17.
54. Glick BS. 2007. Fluorescence microscopy and thin-section electron microscopy. *Methods Mol Biol* 389:251–260. https://doi.org/10.1007/978-1-59745-456-8_18.
55. Walker L, Sood P, Lenardon MD, Milne G, Olson J, Jensen G, Wolf J, Casadevall A, Adler-Moore J, Gow N. 2018. The viscoelastic properties of the fungal cell wall allow traffic of AmBisome as intact liposome vesicles. *mBio* 9:e02383-17. <https://doi.org/10.1128/mBio.02383-17>.
56. Khudyakov JI, Deyarmin JS, Hekman RM, Pujade Busqueta L, Maan R, Mody MJ, Banerjee R, Crocker DE, Champagne CD. 2018. A sample preparation workflow for adipose tissue shotgun proteomics and proteogenomics. *Biol Open* 7:bio036731. <https://doi.org/10.1242/bio.036731>.
57. Heiss S, Maurer M, Hahn R, Mattanovich D, Gasser B. 2013. Identification and deletion of the major secreted protein of *Pichia pastoris*. *Appl Microbiol Biotechnol* 97:1241–1249. <https://doi.org/10.1007/s00253-012-4260-4>.